Photosynthesis Research
https://doi.org/10.1007/s11120-020-00794-z

ORIGINAL ARTICLE

Natural variation in the fast phase of chlorophyll *a* fluorescence induction curve (OJIP) in a global rice minicore panel

Naveed Khan[1,2] · Jemaa Essemine[2] · Saber Hamdani[2] · Mingnan Qu[2] · Ming-Ju Amy Lyu[2] · Shahnaz Perveen[2] · Alexandrina Stirbet[3] · Govindjee Govindjee[4] · Xin-Guang Zhu[2]

Received: 11 May 2020 / Accepted: 26 October 2020
© Springer Nature B.V. 2020

Abstract

Photosynthesis can be probed through Chlorophyll *a* fluorescence induction (FI), which provides detailed insight into the electron transfer process in Photosystem II, and beyond. Here, we have systematically studied the natural variation of the fast phase of the FI, i.e. the OJIP phase, in rice. The OJIP phase of the Chl a fluorescence induction curve is referred to as "fast transient" lasting for less than a second; it is obtained after a dark-adapted sample is exposed to saturating light. In the OJIP curve, "O" stands for "origin" (minimal fluorescence), "P" for "peak" (maximum fluorescence), and J and I for inflection points between the O and P levels. Further, F_o is the fluorescence intensity at the "O" level, whereas F_m is the intensity at the P level, and F_v ($= F_m - F_o$) is the variable fluorescence. We surveyed a set of quantitative parameters derived from the FI curves of 199 rice accessions, grown under both field condition (FC) and growth room condition (GC). Our results show a significant variation between *Japonica* (JAP) and *Indica* (IND) subgroups, under both the growth conditions, in almost all the parameters derived from the OJIP curves. The ratio of the variable to the maximum (F_v/F_m) and of the variable to the minimum (F_v/F_o) fluorescence, the performance index (PI_{abs}), as well as the amplitude of the I–P phase (A_{I-P}) show higher values in JAP compared to that in the IND subpopulation. In contrast, the amplitude of the O–J phase (A_{O-J}) and the normalized area above the OJIP curve (S_m) show an opposite trend. The performed genetic analysis shows that plants grown under GC appear much more affected by environmental factors than those grown in the field. We further conducted a genome-wide association study (GWAS) using 11 parameters derived from plants grown in the field. In total, 596 non-unique significant loci based on these parameters were identified by GWAS. Several photosynthesis-related proteins were identified to be associated with different OJIP parameters. We found that traits with high correlation are usually associated with similar genomic regions. Specifically, the thermal phase of FI, which includes the amplitudes of the J–I and I–P subphases (A_{J-I} and A_{I-P}) of the OJIP curve, is, in turn, associated with certain common genomic regions. Our study is the first one dealing with the natural variations in rice, with the aim to characterize potential candidate genes controlling the magnitude and half-time of each of the phases in the OJIP FI curve.

Keywords Amplitude and kinetics of OJIP curves · Chlorophyll *a* fluorescence · GWAS · JIP test · Natural variation · Photosynthesis

Abbreviations

βGlu-5	*Oryza sativa* 1 β-Glucosidase 5
Chl	Chlorophyll
FI	(Chlorophyll *a*) fluorescence induction
F_o	Basal (initial, minimal) level of chlorophyll *a* fluorescence
F_m	Maximal level of chlorophyll *a* fluorescence
F_v	Variable chlorophyll *a* fluorescence, calculated as $F_v = F_m - F_o$
FC	Field condition

Since 2019 Govindjee uses Govindjee Govindjee as his legal name.

Electronic supplementary material The online version of this article (https://doi.org/10.1007/s11120-020-00794-z) contains supplementary material, which is available to authorized users.

✉ Xin-Guang Zhu
zhuxg@sippe.ac.cn

Extended author information available on the last page of the article

Published online: 07 November 2020

GC	Growth room condition
GWAS	Genome-wide association study
LED	Light emitting diode
OJIP transient	Fast phase of chlorophyll *a* fluorescence induction, where O is for F_o, P is for peak (equivalent to F_m in saturating light), J and I are for inflections between O and P
RMCP	Rice minicore panel
Q_A	The first quinone electron acceptor of Photosystem II (it is a one-electron acceptor)
Q_B	The second quinone electron acceptor of Photosystem II (it is a two-electron acceptor)
PQ	(Mobile) plastoquinone
PS	Photosystem
SNP	Single-nucleotide polymorphism

Introduction

Chlorophyll (Chl) *a* fluorescence induction has been used widely to probe photosynthetic processes since its discovery by Kautsky and Hirsch (1931). Upon illumination by high intensity continuous light, leaves of plants, algae and cyanobacteria show a characteristic polyphasic Chl *a* fluorescence induction curve, termed as the OJIPSMT transient (Strasser and Govindjee 1992; Papageorgiou and Govindjee 2004), during which the fluorescence emitted by photosystem II (PSII) is predominant and variable, while the contribution of PSI fluorescence is minor and practically constant (see e.g., Genty et al. 1990; Govindjee 1995; Pfündel 1998). Although the fast OJIP phase of the transient takes less than one second and represents a minor fraction of the energy absorbed by leaves, it contains rich information about photosynthesis (Goedheer 1972; Schreiber and Vidaver 1976; Govindjee et al. 1986). Its physical basis has been studied extensively, using the so-called JIP test, which includes a set of parameters describing characteristics of both photosystems I and II, but, especially of PSII (Strasser et al. 2000, 2004; Stirbet and Govindjee 2011). The commonly used OJIP parameters include the maximum quantum yield of PSII (inferred from the ratio of variable to maximal fluorescence, F_v/F_m), the apparent light energy absorbed per active PSII reaction center (ABS/RC), and the performance index (PI_{abs}); these have been widely used to investigate the function of photosynthetic systems under different environmental conditions, or between different species (e.g., Guo and Tan 2015; Oukarroum et al. 2016; Kalaji et al. 2014, 2017; Goltsev et al. 2016; Stirbet et al. 2018).

Chl *a* fluorescence induction (FI) is extremely sensitive to variations in electron transfer reactions on either or both (donor and acceptor) sides of PSII (Neubauer and Schreiber 1987; Schreiber and Neubauer 1987; Strasser et al. 1995; Bukhov et al. 2004). Initially, when light first excites dark-adapted photosynthetic samples, the primary quinone electron acceptor (Q_A) is usually in the oxidized state in all the PSII reaction centers, FI has its initial value F_o at the step O, which is light emitted from the antenna, when all the PSII reaction centers are "open" (i.e., with oxidized Q_A; Butler 1978). When the light intensity is high enough to completely reduce all the electron carriers in the linear electron transport chain, Chl *a* fluorescence, during FI, subsequently rises to its maximal level (F_m) at the peak *P*, where all the PSII reaction centers are closed. When FI is plotted on a logarithmic scale, three distinct phases are observed, which include two intermediate steps, J and I. All the three (i) O–J; (ii) J–I; and (iii) I–P phases are affected by the sequential progressive reduction of electron transfer intermediates in PSII, cytochrome (Cyt) b_6/f complex, and in PSI, up to ferredoxin (*F*d), since the ferredoxin–$NADP^+$-reductase (FNR) in plants is inactive 1–2 s after the onset of illumination (see e.g., Schansker et al. 2005). The O–J phase is controlled by photochemical charge separation that leads to Q_A reduction (see Neubauer and Schreiber 1987; Strasser et al. 1995), but the fluorescence yield at and around the J-step may also be affected by the electron donor side of PSII, "the water oxidation clock", i.e., the "oxygen evolving cycle" (involving the transitions of the so-called S states: S0 to S4). The accumulation of S2 and S3 states has been suggested to lead to the quenching of Chl *a* fluorescence near the J-step (Delosme and Joliot 2002; Lazár 2003; Schansker et al. 2011). Indeed, under very high illumination, a transient increase in the concentration of $P680^+$ population (the oxidized primary donor of PSII) is possible during the S2-to-S3 and S3-to-S4-to-S0 transitions, due to a transient limitation on the PSII donor side, and $P680^+$ is a well-known Chl fluorescence quencher (see e.g., Butler 1972; Shinkarev and Govindjee 1993). The O–J phase is the photochemical phase; however, the J–I and I–P phases are parts of the thermal phase of FI, since they involve temperature-dependent steps (see a review by Stirbet and Govindjee 2012). The J–I and I–P phases have been associated with the reduction of all the electron carriers in the electron transport chain between the two photosystems (Schreiber 1986). However, besides the PQ pool reduction, this process also includes the reduction of plastocyanin (PC) via the Cyt b_6/f: this occurs at the end of the J–I phase and at the beginning of the I–P phase, while the (electron) acceptor side of PSI (up to Fd) is reduced at the end of the I–P phase; this is due to a transient bottleneck starting at the FNR level (see e.g., Munday and Govindjee 1969; Satoh 1981; Schansker et al. 2003, 2006). At sub-zero temperatures (< -35 °C), the JIP thermal phase indeed disappears (Neubauer and Schreiber 1987).

In addition to the JIP test (Strasser et al. 2000), Pospisil and Dau (2000) have developed a method to quantitatively analyze the OJIP curves in terms of the amplitudes of each phase and their kinetics by deconvoluting the FI curve into

a sum of three first-order kinetic equations corresponding to the O–J, J–I, and I–P phases of the OJIP curve. This approach was possible since the rate limitations that define these three steps are significant. Although there is still no consensus on the detailed mechanistic bases of the different phases of the OJIP transient, yet the OJIP phase has been successfully used to predict photosynthesis parameters (e.g., Mehta et al. 2010; Živčák et al. 2014; Zhang et al. 2015; Kalaji et al. 2014, 2017; Çiçek et al. 2018; Mishra et al. 2020; for caveats, see Stirbet et al. 2018).

In addition to the above-mentioned biophysical and biochemical studies on FI, another method that can be potentially used to study the mechanistic basis of the OJIP FI curve is to mine the genetic basis underlying the FI curve. Previously, quantitative trait loci (QTL) have been systematically mined to establish association between a phenotypic variation and the associated genetic markers (Doerge 2002). Recent advances in genomic sequencing technology offer a much more efficient approach, i.e., genome-wide association studies (GWAS) to mine genomic variations associated with a particular trait. The GWAS method has been much more efficient than the QTL approach, since the former usually includes many more genetic markers, which incorporate a larger number of recombination events than the traditional QTL approach (Brachi et al. 2011). Thus far, GWAS has been used to identify "casual" gene(s) associated with particular traits in agriculture (Yan et al. 2009; Huang et al. 2010, 2012; Brachi et al. 2011; Kump et al. 2011; Tian et al. 2011; Zhao et al. 2011; Schläppi et al. 2017). The objective of our current study is to mine natural variations of the fast phase of the Chl *a* fluorescence induction curve, i.e., the OJIP curve, in a diverse rice germplasm. This analysis is expected to help identify potential traits influencing photosynthesis efficiency. Earlier, natural variations of different JIP test parameters have been studied in several systems (Hao et al. 2012; Herritt et al. 2018; Oyiga et al. 2019; Rapacz et al. 2019; Quero et al. 2020); however, such a quantitative analysis has not been done systematically in rice, as presented here. More importantly, our current work represents the first systematic study in rice on the natural variation and in finding the potential candidate genes controlling the magnitude and half-time for each of the phases of the OJIP curve. We have used here the quantitative analysis method of Pospíšil and Dau (2000); in addition, we also selected five key JIP test parameters following what Kalaji et al. (2014, 2017) and Goltsev et al. (2016) have suggested. Our present study has provided important information for the understanding of natural variations in different OJIP parameters and in the identification of potential traits influencing photosynthesis efficiency. The results of this study not only show differences in the patterns of natural variations between the two subgroups of rice, i.e., *Japonica* and *Indica*, but they also provide a set of potential candidate genes that might be behind the natural variations of the OJIP phases (as shown later, in Table 3, in this paper). Identifying genes associated with natural variation of OJIP phases is expected to facilitate studying the mechanistic basis of the OJIP phases. Considering that some OJIP-related fluorescence parameters are related to crop photosynthetic performance, e.g., F_v/F_m representing the maximum quantum yield of PSII (see e.g., Strasser et al. 2000; Govindjee 2004), identifying genes associated with different parameters derived from the OJIP curves may provide new candidate genes which can be used to improve photosynthesis for better performance in the field.

Materials and methods

Plant material

In this study, we used 199 rice (*Oryza sativa*) accessions, obtained from the Rice MiniCore Panel (RMCP), developed by the United States Department of Agriculture (USDA), which include accessions from 76 countries covering more than 10 geographic regions (Agrama et al. 2010). The RMCP used here was a subset of 1704 of the core collection of the USDA global Gene Bank. The RMCP is only ~ 12% of the global rice core, yet, it includes almost 98% of all genetic variation (Agrama et al. 2010; Li et al. 2010; Wang et al. 2016; Qu et al. 2017). The 199 rice accessions, used here, include six different rice subgroups, with 34 *temperate Japonica* (TEJ), 36 *tropical Japonica* (TRJ), 6 *Aromatic* (ARO), 36 *Australica* (AUS), 68 *Indica* (IND) and 19 *admixture* (Admix). Further, ARO, TEJ and TRJ are classified as *Japonica* (JAP) subspecies, while IND and AUS as *Indica* (IND) subspecies (Li et al. 2010). Detailed information on accession names, IDs of genetic stock of *Oryza sativa* (GSOR), as given by USDA, geographic origin (along with latitude, longitude and country), and varietal groups (subpopulations) are available in the Additional file #1 under Supplementary file 2).

Growth conditions

Rice accessions were transplanted under two different growth environments: field condition (FC) and growth room condition (GC). For the FC, seeds were transplanted in "soil beds" in 2013 in Beijing, China; after 30 days, plants were transferred into 12 L pots that contained commercial peat soil (Pindstrup Substrate 4; Pindstrup Horticulture) and grown out-doors. Experiments were conducted during the last week of July, 2013 (for details, see; Hamdani et al. 2019). In contrast, all the RMCP samples were grown, during 2016, under controlled environmental growth condition, i.e., growth room condition (GC). Seeds were first germinated on wet filter paper in petri-dishes at 28 °C for 5 days. After the emergence of the radical, seeds were transferred

to plastic pots having the same soil as used for FC plants. In the growth room, the temperature was 27 °C during the day cycle of 14 h, and 25 °C during the night cycle of 10 h. The relative humidity was kept at 75% throughout the day and night. Light provided by tungsten lamps was 600 µmol photons m^{-2} s^{-1} at the top of the plants. For each accession, we grew two pots with three plants per pot; to avoid nutrient limitations, water and nutrients were added routinely for the growth of both FC and GC plants.

Measurement of the fast phase of Chl *a* fluorescence induction: the OJIP transient

Measurement of the fast phase of Chl *a* fluorescence induction (FI) was made using a Multi-functional Plant Efficiency Analyzer (M-PEA; Hansatech, King Lynn, Norfolk, UK). Before measurements, plants were kept in darkness overnight; subsequently fully expanded detached leaves, with the petioles dipped in water, were kept in darkness for additional 10 min in the leaf clip of the instrument. After this dark adaptation period, the upper adaxial surface of the detached leaf was exposed to saturating (5000 µmol photons m^{-2} s^{-1}) orange-red (652 nm) actinic light for 0.5 s; this light was from the light emitting diodes (LEDs), provided by the instrument (for further information, see Hamdani et al. 2019).

To minimize the potential compounding effect, caused by differences in the developmental stages, we performed batch-wise measurements; for the 1st as well as the 3rd batch, we did sequential measurements from accession 1 to 199, while for the 2nd and the 4th batch, we measured the FI in the reverse order (i.e., from accession 199 to 1), as described by Hamdani et al. (2019).

Estimation of single-nucleotide polymorphism (SNP) heritability: *ħ2*

To estimate SNP-based heritability (*ħ2*) of FI traits, we used the Genome-wide Complex Trait Analysis (GCTA) software (version 1.25.2; Yang et al. 2011). The 2.3 million filtered SNPs of the minicore population were used as the genetic information for RMCP (Wang et al. 2016). The method used in GCTA includes two steps: generation of a "high-dimensional" genetic kinship matrix for each of the individuals, and then estimating the variance explained by all SNPs by a restricted maximum likelihood analysis of the phenotypes with the genetic relatedness matrix (Yang et al. 2011). The significance of *ħ2* was evaluated by a likelihood ratio test, which was the ratio of the likelihood under the alternative hypothesis (H1, *ħ2* SNP_0) to that under the null hypothesis (H0, *ħ2*SNP = 0). The output file provided the likelihood ratio and its corresponding *p* values (Qu et al.2017).

Derivation of parameters related to FI and its basic analysis

Parameters characterizing the O–J, J–I, and I–P phases

The experimental FI curves were fitted with the sum of three first-order kinetic curves by non-linear regression, using Sigma Plot (SSI, Richmond, CA). See: Boisvert et al. (2006) and Pospíšil and Dau (2000) for further information.

$$F(t) = F_0 + A_{O-J}\left[1 - \exp\left(-k_{O-J}t\right)\right] + A_{J-I}\left[1 - \exp\left(-k_{J-I}t\right)\right] + A_{I-P}\left[1 - \exp\left(-k_{I-P}t\right)\right] \quad (1)$$

where $F(t)$ is for fluorescence at time t, Fo is fluorescence at time zero, A_{O-J}, A_{J-I} and A_{I-P} are amplitudes, and k_{O-J}, k_{J-I} and k_{I-P} are the rate constants for the O–J, J–I and I–P phases. Then, the half-time ($t_{1/2}$) constant for each phase was calculated as $t_{1/2} = 1/k$ where k is the rate constant.

Parameters characterizing the O–J, J–I, and I–P phases

To obtain quantitative values for the parameters from Chl *a* fluorescence induction, we used (1) the entire OJIP curve characterizing separately the O–J, J–I, and I–P phases; (2) specific fluorescence values at certain times in the transient to calculate a set of parameters (called the JIP parameters) for each sample. We note that these JIP parameters are proxies for different characteristics of PSII and of the photosynthetic electron transport, calculated using several fluorescence values from the OJIP curve (see e.g., Strasser et al. 2000, 2004; Stirbet and Govindjee 2011); these are the minimum fluorescence (F_O), the fluorescence at $t = 0.3$ ms of the transient ($F_{0.3\ ms}$), the fluorescence at two intermediate levels (F_J at 2 ms and F_I at 30 ms), and the maximum fluorescence (F_m). Here, besides the normalized complementary area above the OJIP curve (S_m) and the ratio $F_v/F_o = (F_m - F_o)/F_o$, we used the following JIP parameters: the maximum quantum yield of PSII photochemistry, $F_v/F_m = \varphi_{Po}$, the apparent antenna size of an active PSII reaction center, ABS/RC, and the Performance Index, PI_{abs}. The symbols, definitions and meaning of these JIP parameters are described in Table 1.

Calculation of population genetic variation (PGV)

To quantify the genetic variation in the global rice minicore panel, we calculated population genetic variation (PGV), using the formula, given below, as described by Gu et al. (2014):

Table 1 Definition of the JIP fluorescence parameters studied in this work (Strasser et al. 2004; Stirbet and Govindjee 2011)

Technical fluorescence parameters	Definitions
$F_o = F_{0.05\ ms}$	Minimum (initial) fluorescence
F_m	Maximum fluorescence
$F_J = F_{2ms}$	The fluorescence at $t = 2$ ms
$F_v = F_m - F_o$	Maximum variable fluorescence
$V_J = (F_J - F_o)/F_v$	The relative variable fluorescence at $t = 2$ ms
$M_0 = (\Delta V/\Delta t)_0 \approx 4\ ms^{-1} * (F_{0.3\ ms} - F_{0.05\ ms})/F_v$	Initial slope of the O–J fluorescence rise
$S_m = Area/F_v$	Normalized area between the OJIP curve and the line $F = Fm$, which is proportional with the number of components of the electron transport chain
Energy fluxes	
ABS	The photon flux absorbed by all PSIIs
TR	The part of ABS trapped by the active PSIIs that leads to Q_A reduction
ET	The energy flux associated to the electron transport from Q_A^- to the PQ pool
JIP parameters studied in this work	
$TR_0/ABS = \varphi_{Po} = F_v/F_m$	Maximum quantum yield of PSII photochemistry
$ABS/RC = (M_0/V_J)/\varphi_{Po}$	Apparent antenna size of an active PSII
$PI_{abs} = (RC/ABS) * [\varphi_{Po}/(1-\varphi_{Po})] * [\psi_{Eo}/(1-\psi_{Eo})]$,where:	Performance index on absorption basis
$\psi_{Eo} = 1 - V_J = ET_0/TR_0$	Probability that a trapped exciton moves an electron into the electron transportchain beyond Q_A

These parameters are used to analyze the OJIP phase of Chl *a* fluorescence induction, where O is for origin (the minimum fluorescence F_o), J and I are for two intermediate levels at 2 ms and 30 ms (F_J and F_I), and P is for peak (F_P, or F_m when the fluorescence is maximal). Note that PSII, RC, and Q_A are for photosystem II, the total number of active PSII reaction centers in the measured area, and the first plastoquinone electron acceptor of PSII, respectively

$$PGV = \left(\left(X_{max} - X_{min}\right)/X_{mean}\right)100 \quad (2)$$

where X_{max} is the maximum value, X_{min} is the minimum value and X_{mean} is the mean value in the population.

The R statistical package (https://www.r-project.org) was used to evaluate Pearson Correlation Coefficient between different traits derived from the FI curve (Corrplot; Version 3.2.1).

Genome-wide association studies

For association mapping, 2.3 M bi-allelic SNPs were used having minor allele frequency (MAF) ≥ 5%. Initially, phenotypic data were normalized with qq (quantile–quantile) plot norm function by using the following information from the web site: <https://stat.ethz.ch/R-manual/R-devel/library/stats/html/qqnorm.html>. Furthermore, Genome-Wide Association Studies were conducted using the GEMMA software (see <https://www.xzlab.org/software.html>) through Linear Mixed Model (LMM) approach, as implemented in GEMMA. LMM accounts for both the population structure and the kinship (Hoffman 2013). To minimize false positive association rate, the population structure was corrected by the first four components of the principle component analysis, as described by Wang et al. (2009). Permutation strategy was adopted to determine genome-wide significance values; thus, each targeted phenotype was permuted for 200 repetitions and GWAS analysis was performed for each permuted phenotype and a threshold p value of less than 1×10^{-5} was chosen as a significant threshold. Package qqman was used to generate both the Manhattan and the qq plots (Turner 2018). Further details are described in Hamdani et al. (2019). SNPs with p values $< 1 \times 10^{-5}$ for each parameter are ranked as significant loci (i.e., a putative marker significantly associated with the trait). We detected 596 significant loci (SL) for 11 parameters (see Additional file #2, under Supplementary file 3). Since many significant loci (SL) were found to be associated with a particular trait, we clustered multiple SLs that were within 100 kb region to obtain the number of independent association signals for each parameter; within each cluster, the SNP having the lowest p value was selected as an independent GWAS signal and called lead SNP (see Table S1, in the Supplementary file 1, which shows the list of lead SNP for each trait). The linkage disequilibrium (LD) block analysis was performed using Halploview software for the lead SNPs that are common in at least two traits.

Candidate gene list

We compiled a complete list of genes that are in the LD block region harboring the lead SNPs and shared by at least two traits. Moreover, we also listed potential genes that might affect photosynthesis based on gene annotation

analysis, using four different rice databanks, i.e., rice gene annotation project (rice.plantbiology.msu.edu), pubmed (https://www.ncbi.nlm.nih.gov/pubmed), rapdb (https://rapdb.dna.affrc.go.jp), and phytozome (https://phytozome.jgi.doe.gov).

Results

The fast phase of chlorophyll *a* fluorescence induction, the OJIP transient

Figure 1 shows typical FI curves under FC (left) as well as GC (right). Comparing the average FI curves of all the 199 accessions grown under these conditions, we found that *FI* under *FC* showed a higher F_m by ~ 8% compared to that under GC (cf. the "P" level in Fig. 1a with that in Fig. 1b). Even at the subgroup varietal level, we found higher F_m (the P level) by ~ 6.4% for dmix to 11% for AUS under FC as compared to GC (cf. Fig. 1c, d). The IND and JAP varieties show similar OJIP patterns under the two growth conditions, used here, as shown by data on the average minicore population, i.e., JAP had 7.2% higher F_m, while IND had 9% higher F_m under FC compared to GC condition (cf. Fig. 1e, f). Further, JAP varieties showed higher F_m compared to IND varieties (by 4.5% under FC and by 6% under GC); further, JAP had a faster rate of I–P rise as compared to IND varieties under both the growth conditions (cf. Fig. 1e, f).

Correlation between different Chl *a* fluorescence parameters measured for plants grown under field and growth room conditions

Figure 2 shows the Pearson Correlation Coefficient, calculated to evaluate the relationship between different parameters derived from the FI curves. The parameters obtained from plants grown under the two growth conditions were weakly correlated; for instance, the correlation coefficient for F_v/F_m under these two conditions was 0.167 with a p value of 0.02, while the correlation coefficient for F_v/F_o was 0.183 with a p value of 0.012. However, the other significant correlations between the parameters, measured under the two environments (FC & GC), were for $A_{O–J}$, $A_{J–I}$, $A_{I–P}$, Sm and ABS/RC, which ranged from 0.2 to 0.3 with p values < 0.05.

We further evaluated the correlation between different parameters measured under field and growth room conditions. We found relatively weak but significant correlation between the parameters for plants grown under these two conditions. For instance, the normalized area (Sm) above the FI curve in FC was weakly positively correlated with $t_{1/2O–J}$ (half-time of the O–J phase) ($r = 0.239$, p value < 0.001; Fig. 2) for plants grown under GC; further, under FC, $A_{O–J}$ was positively correlated with ABS/RC ($r = 0.249$, p value < 0.01; Fig. 2) for plants grown under GC. When we evaluated correlations between specific parameters under the same growth condition, we found that F_v/F_m and F_v/F_o were highly positively correlated in both FC ($r = 0.98$, p value < 0.001; Fig. 2) and GC plants ($r = 0.97$, p value < 0.001; Fig. 2). In contrast, $A_{J–I}$ and $A_{I–P}$ were highly negatively correlated, with $r = -0.85$ for FC and $r = -0.70$ for GC with p values < 0.001 (see Fig. 2). On the other hand, ABS/RC was highly positively correlated with $A_{O–J}$ ($r = 0.83$ for FC, $r = 0.85$ for GC, p values < 0.001; Fig. 2), but negatively correlated with the performance index (PI_{abs}) (−0.86 for FC, and −0.88 for GC, with p values < 0.001; Fig. 2). Although, under the two conditions (FC & GC), the absolute values of the parameters were different, yet the correlations between different parameters under the same growth condition were maintained.

Variation among individual parameters as obtained from the OJIP curves

There were large variations among different parameters derived from the Chl *a* fluorescence induction, measured under field and growth room conditions (Table 2). Looking at the Population Genetic Variation (PGV) values (see Material & Methods for details), which describe the extent of natural variation for different individual traits (Gu et al. 2014; Qu et al. 2017), we found that for different parameters of the OJIP curve, measured in FC plants, they ranged from 3.3 to 235.4, while for GC plants, they ranged from 5.5 to 176.9. Interestingly, *F*v/*F*m had a minimum PGV value of 3.3 for FC and 5.5 for GC. The PGV value for each individual trait for GC plants was higher than for FC plants, except for two parameters: the amplitude and half-time of I–P phase ($A_{I–P}$ and $t_{1/2I–P}$). The amplitude and half-time of I–P was higher for FC compared to GC (104.12 and 235.35 for FC; 99.07 and 148.74 for GC, respectively, see Table 2). All the above results, taken together, suggest that most of the parameters, related to FI curve, have higher phenotypic variations in the GC over the FC plants (c.f. Table 2). In addition to PGV, SNP-based heritability test provided additional new information since it characterized the level of genetic control over the parameters studied here. Only three traits displayed significant *ħ2* in GC plants; they were: $t_{1/2}$ for the O–J phase, normalized area above FI curve (Sm), and $A_{J–I}$. The *ħ2* for these three parameters were 0.205 with a p value of < 0.001, and 0.09327, and 0.101 with p values of < 0.01. For FC plants, out of the eleven FI parameters measured, six showed significant *ħ2* values: *F*v/F_m, F_v/F_o and S_m had the highest *ħ2* values of 0.322, 0.323 and 0.227, respectively, all with p values

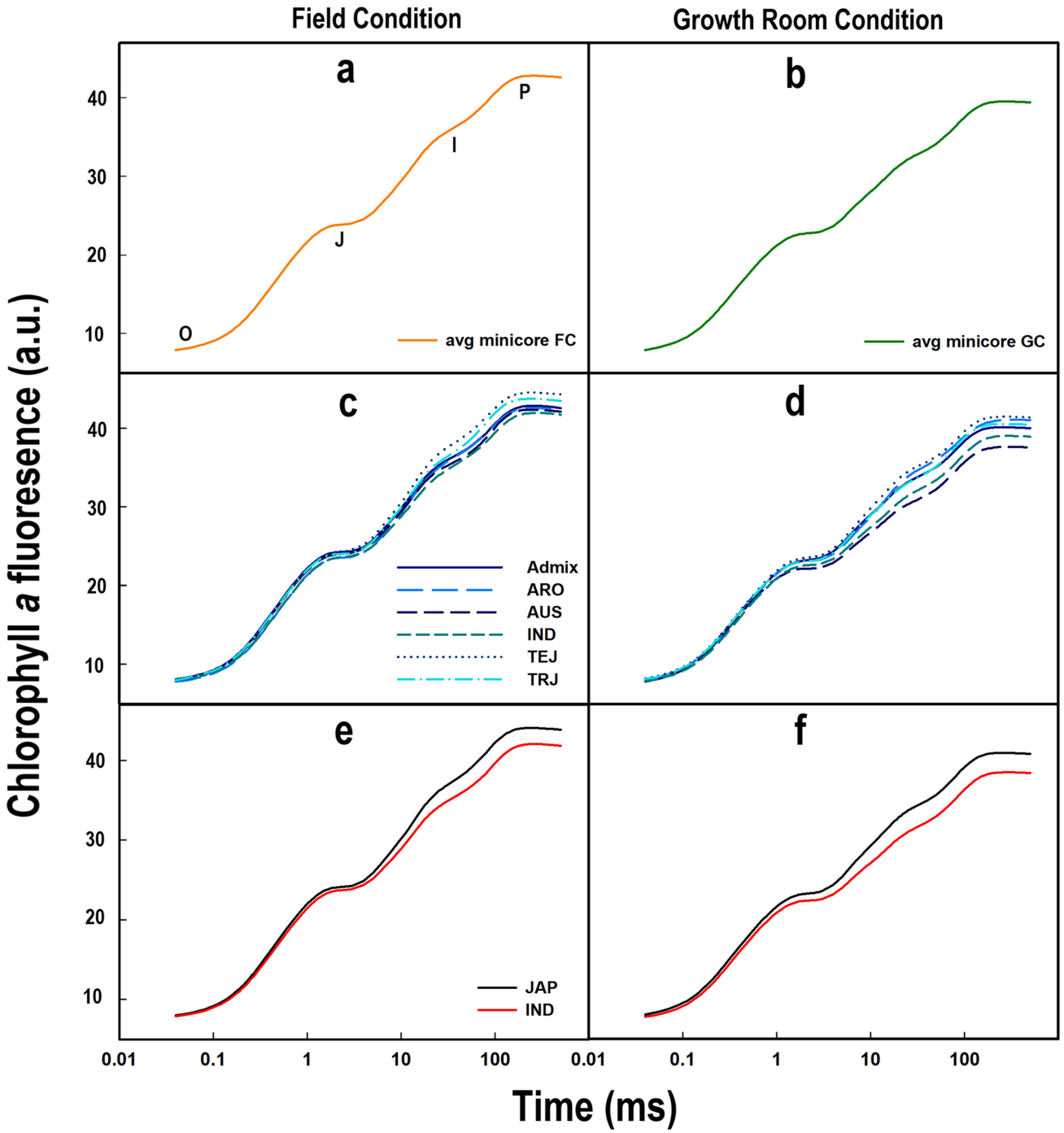

Fig. 1 Natural variation of Chl *a* fluorescence induction curves for rice minicore panel under two different growth conditions. The left three panels **a**, **c** and **e** show the average OJIP curves of 199 rice accession, average OJIP curves of six different subgroup populations and average OJIP curve of subpopulations (IND and JAP), respectively, measured under FC. Similarly, the right three panels **b**, **d** and **f** show the average OJIP curves of 199 rice accessions, average OJIP curves of six different subgroup populations and average OJIP curve two subpopulations (IND and JAP), respectively, measured under GC

of < 0.001; the other three traits (A_{O-J}, $t_{1/2\ I\text{-}P}$ and PI_{abs}; see Table 2) showed somewhat lower, but still significant (p value < 0.001) $\hbar 2$ values. Furthermore, when two-way ANOVA was employed to assess genotype × environment interaction with respect to FI parameters in FC and GC plants, we observed that only two parameters (S_m and

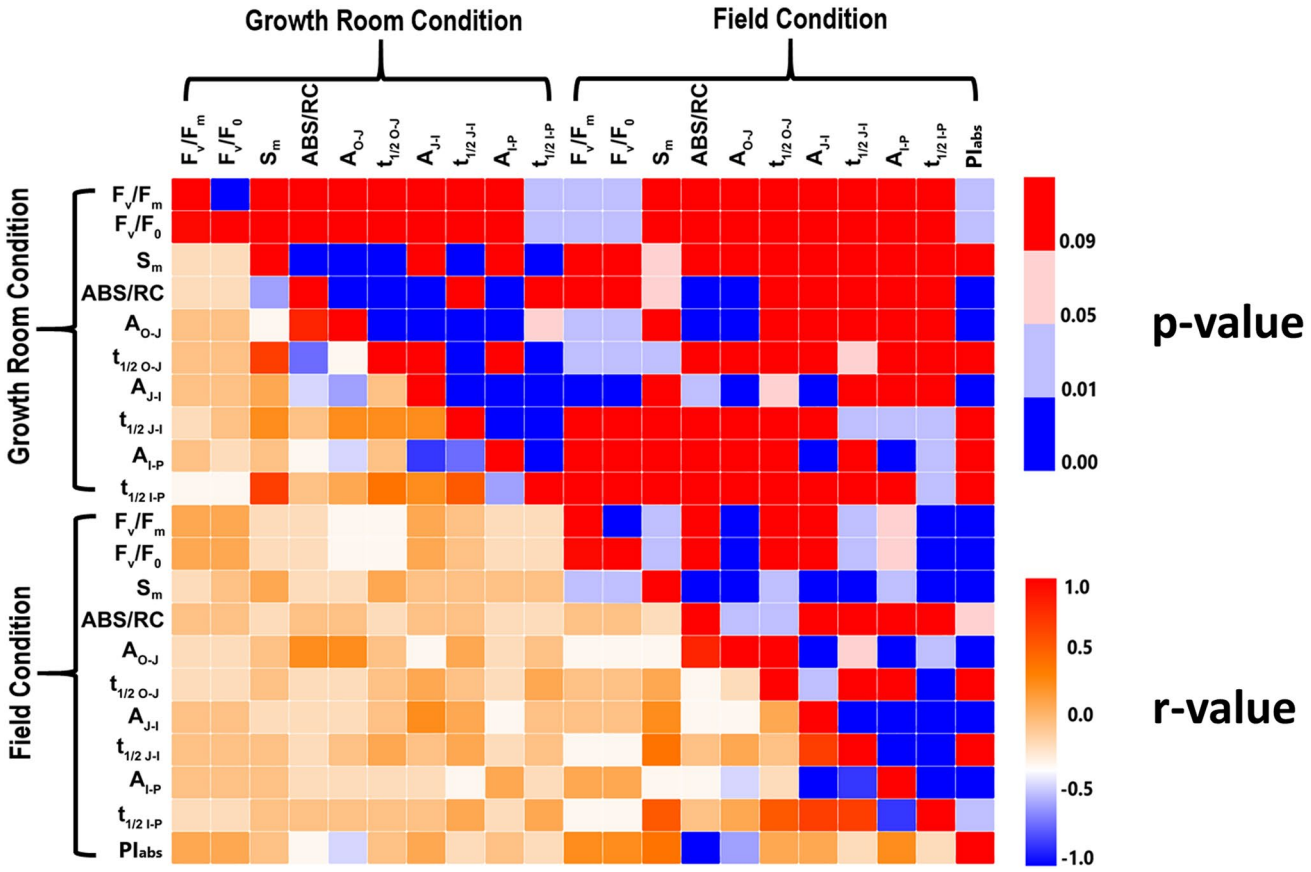

Fig. 2 Matrix of Pearson's Correlation Coefficients (*r*) (Left Triangle) and *p* values (Right Triangle) of fast transient Chl *a* fluorescence parameters under field and growth room conditions. F_v/F_m is the maximum quantum yield, Sm is the normalized area above Chl *a* fluorescence curve, i.e., proportional to the amount of electron acceptors available to PSII, and ABS/RC is the apparent antenna size of an active PSII. Further, the amplitude of each phase ($A_{O–J}$, $A_{J–I}$ and $A_{I–P}$) in Chl *a* fluorescence curve and half-time ($t_{1/2\ O–J}$, $t_{1/2\ J–I}$ and $t_{1/2\ I–P}$) to reach each phase in Chl *a* fluorescence are also shown

Table 2 Percent genetic variation (PGV) and SNP-based heritability (*ħ2*) of fast Chl *a* fluorescence transient traits in the global minicore grown under Field Condition (FC) and Growth Room Condition (GC), along with two-way ANOVA (F ratio and significance determining effect of environment, genotype and environment × genotype interaction for selected Chl *a* fluorescence parameters), are shown below

Traits	PGV (FC)	$\hbar^2$ (FC)	PGV (GC)	$\hbar^2$ (GC)	Genotype (G)	Environment (E)	GxE
F_v/F_m	3.2891	0.32187***	5.4767	0.01194ns	0.901ns	56.437**	1.027ns
S_m	55.0074	0.2275***	103.4144	0.0927**	4.398***	0.029ns	0.457ns
ABS/RC	86.0037	< 0.0001 ns	95.0019	< 0.0001ns	2.889ns	121.482**	3.412ns
$A_{O–J}$	73.0302	0.0578**	76.2835	0.0282ns	1.478ns	1.773ns	1.031ns
$t_{1/2\ O–J}$	33.0875	0.0092 ns	45.9229	0.2050***	0.479ns	5.253ns	0.439ns
$A_{J–I}$	131.3640	0.0109 ns	175.8854	0.1009**	0.652ns	0.842ns	0.473ns
$t_{1/2\ J-I}$	129.3435	0.0147 ns	176.8645	0.0295ns	0.195ns	0.953ns	0.143ns
$A_{I–P}$	104.1214	0.0047ns	99.0711	0.0285ns	186.02***	46,541.3***	11.33*
$t_{1/2\ I–P}$	235.3574	0.0865**	148.7358	0.0094ns	142.0ns	42,085.52 n.s	49.94ns
F_v/F_o	19.3556	0.3226***	N.D	N.D	1.2 ns	11.276*	1.159 ns
PI_{abs}	135.5528	0.0576**	N.D	N.D	ND	ND	ND

ND means parameter not determined. Single, double and triple asterisks, after the numbers, represent different *p*-values: < 0.05 (*); *p*-value < 0.01 (**) and *p*-value < 0.001 (***), while ns means non-significant

$A_{I–P}$) out of 9 were significantly influenced by the genotype, while 4 parameters (i.e., F_v/F_m, ABS/RC, $A_{I–P}$ and F_v/F_o.) were significantly affected by the environment. Moreover, there was only one parameter, $A_{I–P,}$ which was significantly affected by the environment and genotype interaction (Table 2).

Comparison of the parameters obtained from the OJIP curves measured on plants grown under field and growth chamber conditions

When we compared the average amplitude of the O–J phase ($A_{O–J}$) in GC and FC plants, we found a slightly lower (3.1%) value in the latter. Further, the average $A_{J–I}$ in the FC plants was higher (9%) than in the GC plants, for the entire minicore population. On the other hand, the average $A_{I–P}$ was 6% lower in the FC than in the GC plants. However, the sum of these two amplitudes under both these conditions was approximately equal (Fig. 3e, i; also see Fig. S1e and S1i, under Supplementary file 1). This implies that the ratio between the amplitude of the photochemical (i.e., $A_{O–J}$) and the thermal phase (i.e., $A_{J–I} + A_{I–P}$) is more or less constant in these plants.

Comparing the kinetics of the different phases of FI, we observed that in FC compared to GC plants, the average half-time of the O–J ($t_{1/2\ O–J}$) and the J–I ($t_{1/2\ J–I}$) phases were 13.9% and 19% higher for the entire minicore panel, respectively, whereas the average half-time for the I–P ($t_{1/2\ I-P}$) phase was lower (9.6%) (Fig. 3m, q and j; also see Fig. S1m, S1q and S1u in the supplementary file 1). The lower $t_{1/2}$ of the I–P phase under FC indicates that the reduction by PSII of the fraction of the oxidized PQ pool left after the J–I phase is faster in FC than in GC plants, most probably due to a slower simultaneous PQ pool re-oxidation by PSI via Cyt b_6/f; this also explains the lower $A_{I–P}$ in FC than in GC plants (see above). This may also be a result of a lower PSI/PSII ratio in FC, or a lower participation of PSI in the linear electron transport, due to an increased cyclic electron transport. More quantitative measurements are needed to determine the contribution of these different potential mechanisms to the observed difference in $t_{1/2}$ of I–P phase and $A_{I–P}$ under different growth conditions.

Furthermore, in FC plants, we observed that the difference in the amplitudes of either $A_{O–J}$ or $A_{I–P}$ phases between all the subgroups and the subpopulations were quite different, as shown in Fig. 3b, c, j and k. The $A_{O–J}$ was significantly higher (by ~ 4.5%) in all the IND than in the JAP accessions (Fig. 3c); however, the reverse was observed for $A_{I–P}$ (~ 6.6% higher in JAP than in IND) (Fig. 3k). On the other hand, there was no significant difference in the values of $A_{J–I}$ between JAP and IND subpopulations. Furthermore, in GC plants, $A_{O–J}$ and $A_{I–P}$ values were ~ 5% lower in JAP, over IND subpopulation, while the $A_{J–I}$ values were 18% higher in JAP over IND (Supplementary Fig. S1 under supplementary file 1). The value of $t_{1/2}$ for each phase was significantly higher in IND than in JAP under both FC and GC conditions; this may be due to the electron transfer rate beyond PSII being slower in IND than in JAP plants in the entire rice minicore panel (see Fig. 3 and Fig. S1 under supplementary file 1).

Variation of parameters related to the OJIP curves of plants grown under field condition

To gain further insight into the natural variation and, consequentially, the genetic basis of the key parameters directly related to the OJIP transient (i.e., F_v/F_m, Sm, ABS/RC, F_v/F_o and PI_{abs}), we further analyzed these parameters (see Fig. 4), particularly in FC plants, since we had observed here a higher SNP heritability (cf. Table 2).

F_v/F_m, variable to maximum fluorescence, a proxy for the maximum quantum yield of PSII

The average F_v/F_m for 199 rice accessions determined under FC was slightly but significantly higher (by 1.09%, with a p value < 0.001 using student t-test) than that under GC (Fig. 4a and Fig. S2a under supplementary file 1). In FC, the F_v/F_m values of JAP subpopulation (ARO, TEJ and TRJ) were slightly higher (~ 1% with a p value < 0.001) than in IND subpopulation (AUS and IND), while Admix accessions had intermediate F_v/F_m values (Fig. 4b, c). A similar trend for these two groups was observed in the case of GC plants (F_v/F_m was slightly but significantly ~ 0.7% higher with a p value of 0.029 in JAP, compared to IND, cf. Supplementary Fig. S2c in supplementary file 1). These variations in F_v/F_m between different subpopulations are in agreement with those observed earlier by Kasajima et al. (2011).

The normalized area above the OJIP curve: S_m = Area/F_v

The normalized area above the fast phase of Chl *a* fluorescence induction (i.e., S_m = Area/F_v), from the "O" (F_o) to the "P" (F_m) level, is proportional to the number of Q_A turnovers during the OJIP transient, and thus, to the number of electron acceptors of the photosynthetic linear electron transport chain (PETC) (e.g., Strasser et al. 2000; Bennoun 2001). We did not find any significant differences between the normalized area for the plants grown under FC and GC. Furthermore, Fig. 4f shows that all members of RMCP, i.e., Admix, ARO, TEJ, TRJ and AUS had smaller Sm (~ 8%) compared to IND subpopulation. The IND subgroup had the largest Sm, implying that this subgroup has higher number of electron acceptors in PETC; it was 10% higher in IND than in the JAP group, with a p value < 0.001. Just as for the FC plants, summarized above, the same trend was observed also for the GC plants: The Sm for the IND plants was 10.5% higher than in the

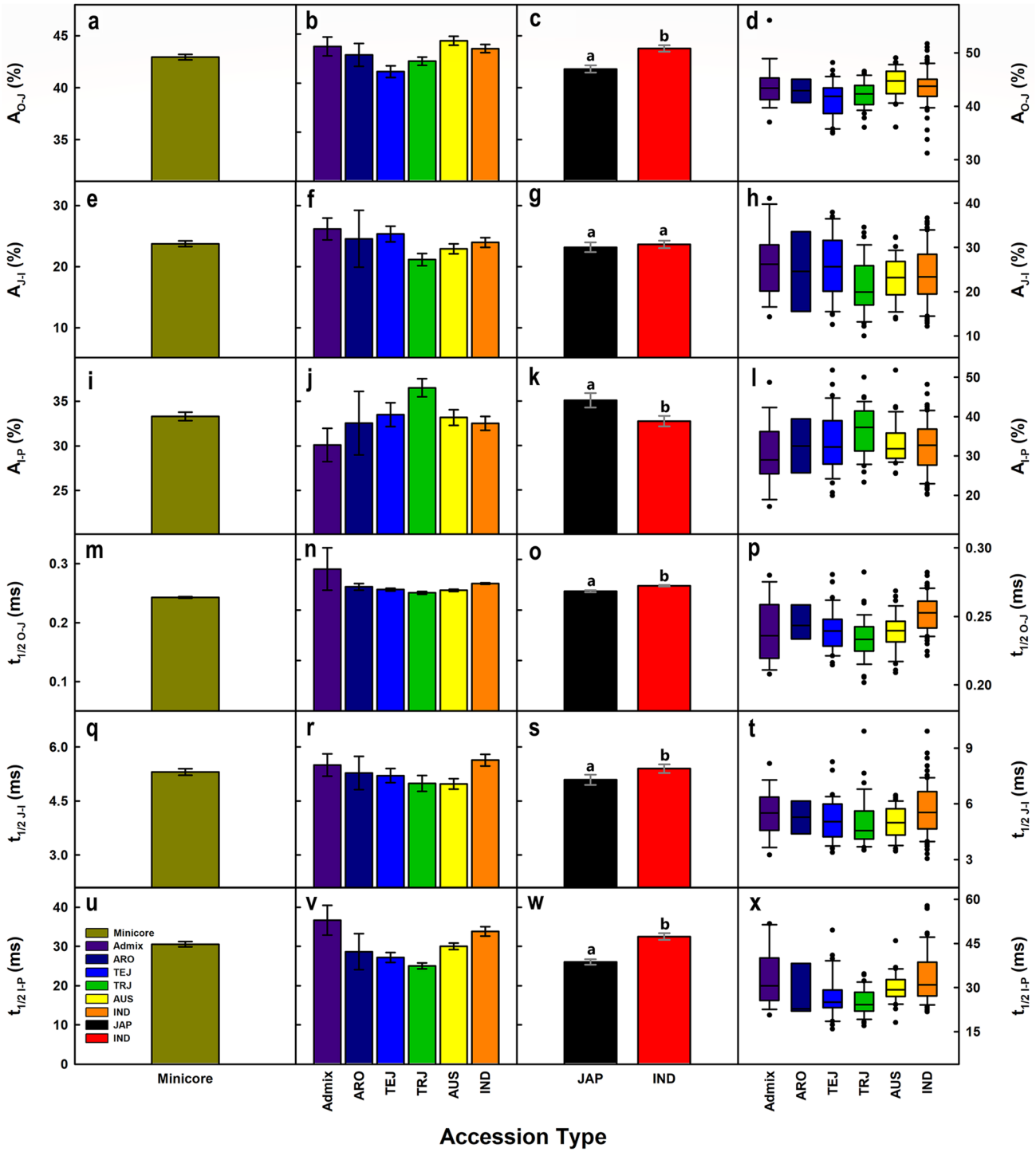

Fig. 3 Phenotypic variations in the kinetic parameters of the OJIP curves. Here are shown phenotypic variations observed for the amplitudes and the half-times of O–J, J–I, and I–P in a diverse germplasm, measured under field condition (for germplasm details, see "Material and Methods"). The first three rows are for the amplitudes and the last three rows are the half-times of O–J, J–I and I–P phases. Columns from Left to Right show: average value of the amplitude and half-time of each of the O–J, J–I and I–P phases, for the whole minicore panel; variation among average values of each parameter for the six subgroup populations; variation between average values of each parameter for the two main subpopulations (IND and JAP); and distribution of each parameter among the whole rice minicore panel. Results are means of 4 replications ($n = 4$); Different lower-case letters indicate significant difference at p value ≤ 0.05

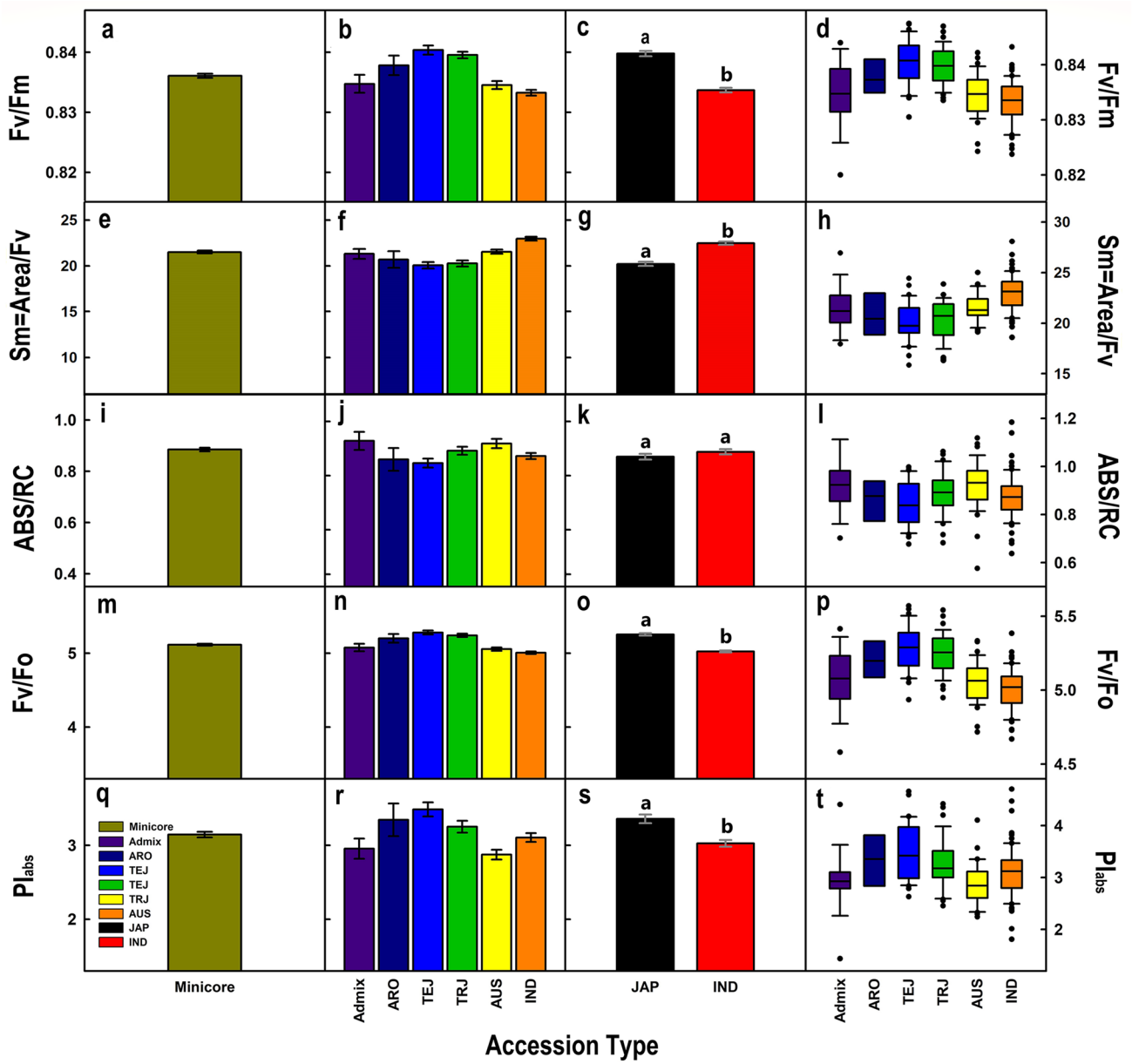

Fig. 4 Phenotypic variation observed for five different JIP parameters in a diverse germplasm measured under field conditions. **a**–**d** F_v/F_m; **e**–**h** S_m; **i**–**l** ABS/RC; **m**–**p** F_v/F_o; and **q**–**t** PI_{abs}. Left to right panels are: for the whole germplasm (dark yellow); for six subgroup populations (color coded, as defined in panel **q**); for the two main subpopulations (IND and JAP, red and black, respectively); and for the distribution of all the parameters (top to bottom) in the 6 subgroup populations. Results are the mean of 4 replications ($n=4$), Different lower-case letters indicate significant difference at p value ≤ 0.05

JAP plants (Fig. 4g and Fig. S2g under supplementary file 1).

Apparent antenna size of an active PSII: ABS/RC

ABS/RC is the ratio of the energy flux absorbed (i.e., ABS) by all PSIIs to the number of active PSII reaction centers (i.e., RC), which is a measure of the apparent antenna size of an active PSII. The average value of ABS/RC for all 199 rice accessions was 0.8849 ± 0.1008 for FC (Fig. 4i) and 1.1141 ± 0.0203 for GC plants (Fig. S2i, supplementary file 1). The relatively larger PSII antenna size for plants grown under GC might be due to the lower light condition for the GC compared to the FC plants (Yang et al. 2007; Tsai et al. 2019). We, however, note that there was no significant difference between the antenna size of JAP and IND populations (c.f. Fig. 2k).

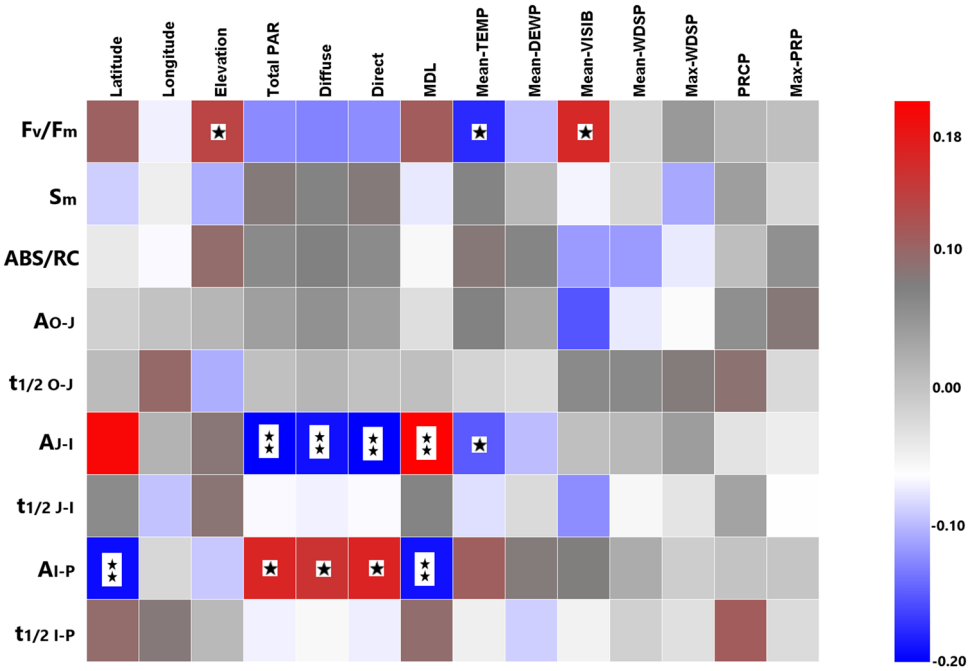

Fig. 5 Heat Map for selected fluorescence transient parameters measured under field condition with global minicore natural habitat climate conditions. The climate parameters included are: longitude, latitude, elevation, mean photosynthetic active radiation (PAR), maximum day length (MDL), mean temperature, mean dew point (DEWP), mean visibility (VISIB), mean wind speed (WDSP), maximum wind speed (WDSP), rain fall or precipitation rate (PRP), and maximum precipitation rate (PRP_{max}). For the y-axis parameters, see the top of the figure (cf. Fig. 2). The colors in cells ranging from red to blue represent the correlation coefficient from negative to positive, while the single asterisk ("*") depicts a p value of <0.05, and the double ("**") asterisks of 0.01

F_v/F_o, reflecting k_P/k_N

The ratio F_v/F_o is equal to the ratio k_P/k_N (see e.g., Tsimilli-Michael 2020); here, k_P is the photochemical de-excitation rate constant, and k_N is the non-photochemical de-excitation rate constant of PSII (mainly heat dissipation, which is essentially constant during the OJIP transient). Thus, since $F_v/F_m = k_P/(k_N + k_P)$ (see e.g., Strasser et al. 2000), this explains the strong correlation between these two parameters observed in this study. On the other hand, F_v/F_o was 5.9% higher in the FC than in the GC plants (cf. Fig. 4n, o; also see Figs. S2n and S2o under supplementary file 1 for FC and GC, respectively). The JAP group showed higher (by 4.5% for FC and 2% for GC) F_v/F_o values compared to the IND group. Figure 4p (also see Fig, S2p under supplementary file 1) shows the distribution of F_v/F_o values for all the six subgroup populations (see Fig. 4 for the names) under FC and GC.

Performance index: PI_{abs}

PI_{abs} is a consolidated parameter, which includes three individual JIP parameters (see Stirbet et al. 2018): (i) the apparent antenna size of an active PSII (ABS/RC); (ii) the likelihood that an absorbed photon can be trapped by PSII RCs ($F_v/F_m = \varphi_{Po}$); and (iii) the efficiency with which electrons are transferred beyond Q_A in the electron transport chain (ψ_{Po}) (see Eq. 3), and Table 1 (under "Material and Methods").

$$PI_{abs} = RC/ABS * (\varphi_{Po}/(1-\varphi_{Po}) * (\psi_{Po}/(1-\psi_{Po}) \quad (3)$$

The average PI_{abs} value for the entire minicore panel under FC was 3.14 ± 0.52. There was a substantial variation in PI_{abs} between different subgroups; members of the JAP group (ARO, TEJ and TRJ) had significantly higher PI_{abs} values (by ~ 11%) than the IND group (IND and AUS) (see Fig. 4r, s). Figure 4u shows the distribution of PI_{abs} values among all the subpopulations used here; we note that the values of PI_{abs} for the members of the IND subgroup have the greatest spread among all the rice accessions used in this work.

Correlation of Chl *a* fluorescence parameters with natural habitat and climate conditions where the plants were grown

Figure 5 shows a heatmap of the correlation (blue for negative; red for positive) between the parameters derived from

Chl *a* FI curves measured for the entire RMCP, under FC with the climatic conditions of their origin.

We note that the amplitude of the J–I phase (A_{J-I}) and that of the I–P phase (A_{I-P}) are significantly correlated with their natural habitat climate conditions, especially for light and temperature. On the other hand, A_{J-I} is negatively correlated with the Photosynthetically Active Radiation (PAR) and with the mean temperature, whereas it is positively correlated with the latitude. However, A_{I-P} shows a reverse correlation with PAR and temperature (Fig. 5). For plants growing under GC, the same correlation between A_{J-I} with PAR and of A_{J-I} with mean temperature is found; however, instead of A_{I-P}, A_{O-J} is seen to be significantly correlated with their original PAR, and the mean temperature (see Fig. S3, under supplementary file 1). In addition to the above, the maximum quantum yield of PSII (inferred from *F*v/*F*m) shows a negative correlation with the mean temperature and PAR in the natural habitats of the plants; F_v/F_m also shows a positive correlation with their mean visibility (VISIB) in FC plants. As expected, we note that the PAR and temperature are two major environmental factors that show strong correlation with the parameters derived from Chl *a* FI.

Genome-wide association analysis of the parameters derived from the OJIP curve

Table 2 shows that most of the FI parameters measured on plants, grown under GC, have no statistically significant *ħ2* except for Sm, A_{J-I} and $t_{1/2}$ of the O–J phase, with values of 0.0927**, 0.1009** and 0.2050***, respectively. On the other hand, 6 out of 11 parameters from FI, measured on plants under FC, showed statistically significant *ħ2* values in the range of 0.05** to 0.32*** (see Table 2).

We now present results from GWAS on the parameters related to FI, measured on FC plants, using the GEMMA software (see details under "Material and Methods"). Here, we have used 2.3 million SNPs with a minor allele frequency (MAF) > 0.05 for association analysis; further, a permutation analysis was conducted to set the suggested threshold. Note that we set a threshold value of $-\log10$ (*p* value) > 5 to identify putative markers associated with specific traits; further, SNPs exceeding the threshold value were considered as a significant loci (SL) showing association with a trait. We detected a total of 596 SLs for all the eleven Chl *a* FI parameters (see additional file #2, in the Supplementary file 3). We found that many SLs are shared between multiple traits, e.g., F_v/F_m and F_v/F_o shared 39 common SLs (*r*-value = 0.98); similarly, ABS/RC and PI_{abs} shared 53 common SLs, and ABS/RC and Sm shared 4 common SLs. Finally, the A_{J-I} and A_{I-P} shared 7 SLs, and, one common SL was found between A_{J-I}, A_{I-P} and $t_{1/2}$ of I–P.

Following Wang et al. (2015), we shortlisted the SLs by clustering multiple SLs for each 100 kb region and the putative marker; the lowest *p* value in the cluster was chosen as the lead SNP. Following this method, we obtained 58 lead SNPs from 342 SLs of the JIP test parameters. Moreover, 41 lead SNPs were decoded from 254 SLs of quantitative traits. Finally, a total of 99 lead SNPs were obtained for the eleven OJIP traits from our GWAS study (for details, see Table S1 under supplementary file 1, for lead SNPs).

Table 3 List of the most significant signals for each parameter along with the SNP location, with their corresponding *p* value

Traits	Most significant *p* value	Chromosome	Most significant SNP position
F_v/F_m	9.53E−08	Chr1	Chr1-40840545
ABS/RC	1.88E−07	Chr9	Chr9-7043571
S_m	1.49E−09	Chr1	Chr1-24940581
F_v/F_o	1.20E−07	Chr1	Chr1-40840545
PI_{abs}	2.12E−08	Chr9	Chr9-7048280
A_{O-J}	7.66E−06	Chr6	Chr6-4756147
$t_{1/2\ O-J}$	9.81E−08	Chr7	Chr7-25428218
A_{J-I}	8.44E−07	Chr1	Chr1-4048849
$t_{1/2\ J-I}$	1.80E−07	Chr8	Chr8-27232545
A_{I-P}	1.06E−06	Chr1	Chr1-4048102
$t_{1/2\ I-P}$	2.17E−06	Chr8	Chr8-3232408

Table 3 shows the most significant putative marker for all the 11 traits. It is obvious from Fig. 6 and Table 3, that GWAS has identified similar genomic regions for highly correlated parameters. In this study, the most significant SNPs for F_v/F_m and F_v/F_o traits have been found to be identical, i.e., Chr1-40840545, with *p* values of 9.53×10^{-08} and 1.20×10^{-07}, respectively (Fig. 6a, b). Similarly, ABS/RC and PI_{abs}, having most significant SNPs, lying within chromosome 9, seems to appear within 5 kb region as Chr9-7043571 and Chr9-7048280, with *p* values of 1.88×10^{-07} and 2.11×10^{-08}, respectively (see Fig. 6c, d).

Furthermore, the most significant GWAS signals for A_{J-I} and A_{I-P} traits were identified within chromosome 1 (Chr1-4048849, having a *p* value of 8.44×10^{-07}, and Chr1-4048102, having a *p* value of 1.06×10^{-06}) (see Fig. 6e, f). The most significant GWAS signal in all of the eleven traits was obtained for Sm (the normalized area above the OJIP curve) (see Table 3), in chromosome Chr1-24940581, with a *p* value of 1.49×10^{-09}. See also Fig. S4 under supplementary file 1 containing Manhattan plots for all the remaining 5 Chl *a* fluorescence parameters (for a background, see Gibson 2010).

The genes known to be related to photosynthesis in the same linkage disequilibrium (LD) block, which harbors a lead SNP, and is considered common for two traits, are listed in Table 4. The identified genes were annotated based on the information from the following four different databases: rice gene annotation project (rice.plantbiology.msu.edu), pubmed (https://www.ncbi.nlm.nih.gov/pubme

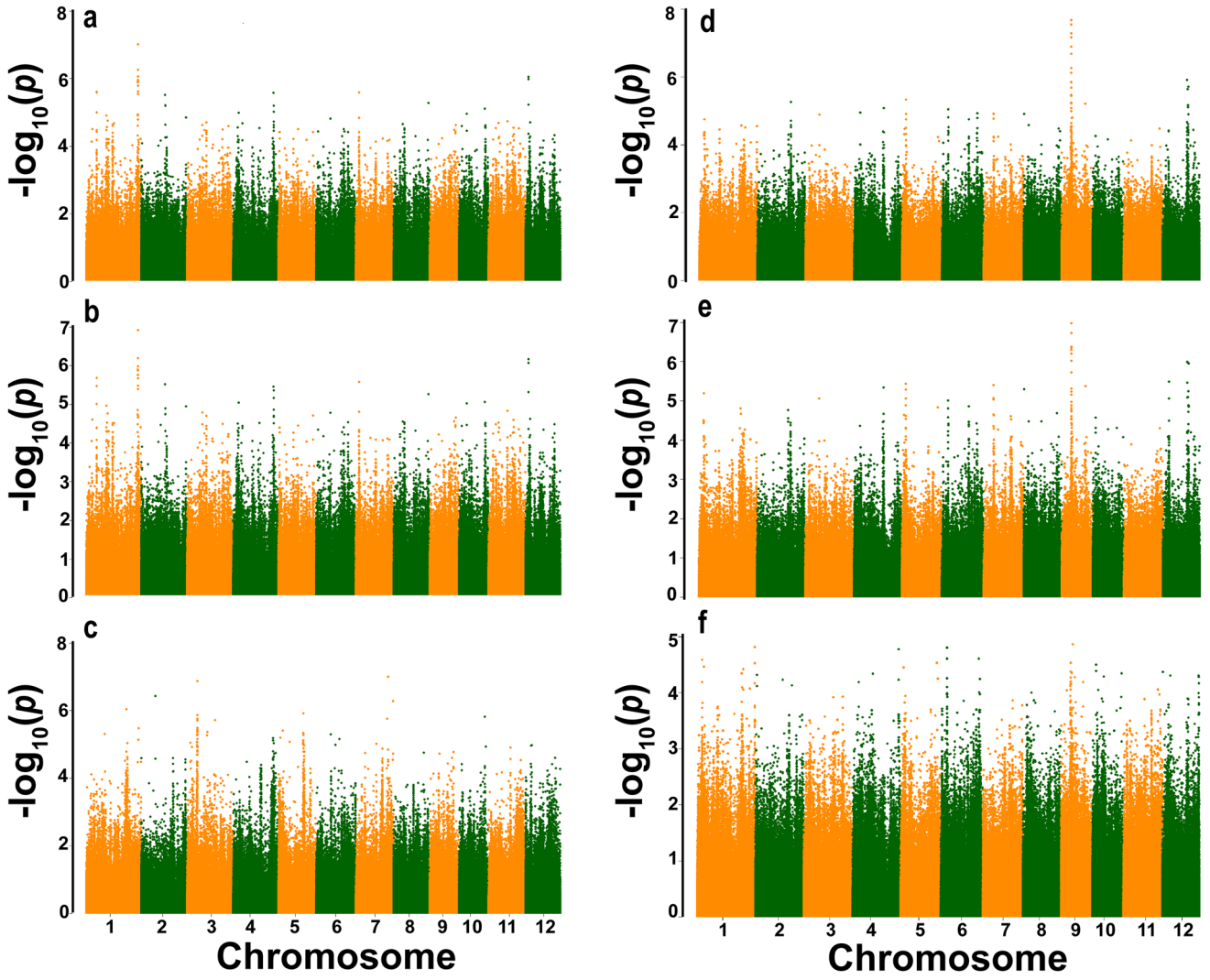

Fig. 6 Manhattan plot of Chl *a* fluorescence parameters having common lead SNPs for at least two traits under field environment. Each point signifies one SNP over 12 rice chromosomes, with their chromosomal position on the x-axis and its associated $-\log_{10}(p$ value) on the y-axis. **a** F_v/F_m; **b** F_v/F_o; **c** A_{J-I}; **d** ABS/RC; **e** PI_{abs}; and **f** A_{I-P}

d), rapdb (https://rapdb.dna.affrc.go.jp), and phytozome (https://phytozome.jgi.doe.gov). The selection of these genes is based on *gene ontology* and *GO analysis*; out of 9 candidate genes, two genes are associated with PSII, one gene is a subunit of PSI reaction center (PsaK), and one gene is a subunit of NDH subcomplex. Moreover, one of the genes is directly related to a part of the light harvesting complex, while another gene is annotated as being involved with electron transport chain, and two remaining genes are involved in gibberellic acid (GA) signaling pathway, and finally one gene is involved in auxin-responsive pathway. In addition to all this, we also provide here a complete list of the genes appearing in the LD block region of the shared lead SNP (see Table S2 under supplementary file 1).

Discussion

Chl *a* fluorescence induction (FI) curves have been used widely to study photosynthetic energy and electron transfer processes among the two photosystems (see e.g., Govindjee 1995; Stirbet and Govindjee 2011, 2012). The FI includes both a fast OJIP induction phase and a slow PSMT phase (Govindjee 1995; Papageorgiou and Govindjee 2011; Stirbet and Govindjee 2016). Variations of the FI curve reflect changes in the energy and electron transfer processes among the photosystems. Thus far, the variation of FI under different treatments, either external environmental stress, or internal genetic manipulation has been extensively studied (see e.g., Dai et al. 2009; Sun et al. 2009; Kalaji et al. 2012, 2014; Zhu et al. 2005; Goltsev et al. 2016; Driever et al. 2017;

Table 4 List of possible candidate genes associated lead SNP found common with more than one parameter

Classification	MSU ID	Trait	Annotation	RAPDB_description	NCBI_description	GO-description
PS II	LOC_Os01g71190	F_v/F_m F_v/F_o,	Photosystem II protein Psb28, class 1 domain containing protein	Photosystem II protein Psb28, class 1 domain containing protein	photosystem II reaction center PSB28 protein, chloroplastic-like	Biological Process: photosynthesis (GO:0015979), Cellular Component: photosystem II (GO:0009523)
	LOC_Os07g05360	F_v/F_m F_v/F_o	Similar to Photosystem II 10 kDa polypeptide, chloroplast precursor	Similar to Photosystem II 10 kDa polypeptide, chloroplast precursor	Photosystem II 10 kDa polypeptide, chloroplastic	Biological Process: photosynthesis (GO:0015979), Cellular Component: photosystem II
PS I	LOC_Os07g05480	F_v/F_m F_v/F_o	Photosystem I protein-like protein	Photosystem I protein-like protein	Photosystem I reaction center subunit psaK, chloroplastic	Biological Process: photosynthesis (GO:0015979), Cellular Component: photosystem I (GO:0009522)
Photosynthetic NDH	LOC_Os01g70400	F_v/F_m F_v/F_o	Conserved hypothetical protein.; Similar to predicted protein.; Similar to predicted protein	NA	Photosynthetic NDH subunit of subcomplex B 5, chloroplastic	NA
Light harvesting complex	LOC_Os09g12540	ABS/RC PI_{abs}	Chlorophyll a-b binding protein family protein	Chlorophyll a-b binding protein family protein	Chlorophyll a-b binding protein 7, chloroplastic	Biological Process: photosynthesis, light harvesting (GO:0009765), Cellular Component: membrane (GO:0016020)
Electron transport	LOC_Os07g05400	F_v/F_m F_v/F_o	Similar to Ferredoxin-NADP reductase precursor (Fragment).; Similar to Ferredoxin–NADP reductase	Ferredoxin–NADP reductase, embryo isozyme, chloroplastic-like		Biological Process: oxidation–reduction process (GO:0055114), Cellular Component: thylakoid membrane (GO:0042651), Molecular Function: ferredoxin-NADP + reductase activity (GO:000324)

Table 4 (continued)

Classification	MSU ID	Trait	Annotation	RAPDB_description	NCBI_description	GO-description
Other	LOC_Os01g70520	F_v/F_m F_v/F_o	Os1bglu5—beta-glucosidase homologue, similar to G. max isohydroxyurate hydrolase, expressed	NA	NA	NA
	LOC_Os01g08320	A_{J-I} A_{I-P}	OsIAA1—Auxin-responsive Aux/IAA gene family member, expressed	A member of rice Aux/IAA family, Cross-talk of auxin and brassinosteroid signaling pathways, Plant morphogenesis	Auxin-responsive protein IAA1-like	Molecular Function: protein binding (GO:0005515)
	LOC_Os01g08220	A_{J-I} A_{I-P}	Gibberellin 3-beta-dioxygenase 2–2, putative, expressed	GA 3 beta-hydroxylase2, GA metabolism	Gibberellin 3-beta-dioxygenase 2–3	Biological Process: oxidation–reduction process (GO:0055114), Molecular Function: oxidoreductase activity, acting on paired donors, with incorporation or reduction of molecular oxygen, 2-oxoglutarate as one donor, and incorporation of one atom each of oxygen into both donors (GO:0016706)

Stirbet et al. 2018; Jimenez-Francisco et al. 2019; Wungrampha et al. 2019). Furthermore, variations of FI curves, under different stresses, and that too among different cultivars, for instance of maize, barely and rice, have been reported (see e.g., Yang et al. 2007; Kalaji et al. 2014; Živčák et al. 2015; Goltsev et al. 2016; Tsai et al. 2019). These data show that there are also large genetic variations of FI curve within the same species. All this information clearly implies the existence of a largely unexplored resource to tap into to gain new insights into the mechanisms of photosynthetic energy and electron transfer. Our current study clearly demonstrates that (1) there are large genetic variations in the fast phase of the FI induction curves, including those in their related quantitative parameters; (2) many of these parameters are influenced not only by total incident PAR, but also by temperature; (3) many of the measured (or calculated) parameters are under strong genetic control and hence are amenable for genome-wide association study. Finally, with the genomic sequence information available, we have conducted an initial analysis and have identified candidate linkage disequilibrium blocks for each independent signal appearing in more than one parameter, which, indeed, can be used later for the purpose of gene identification. Here, we briefly discuss the major findings of this current study.

Natural variation of FI-related parameters

To study the natural variation in FI-related parameters under different environmental conditions, we have measured FI curves under two different growth environments (field, and growth room), using a rice minicore diversity panel, which is a representative subset of 1704 global rice core collection (Agrama et al. 2010; Li et al. 2010). First, we found that the trends in different parameters among different subgroups were similar between the two growth conditions used here (Fig. 2). In this study, our aim was to quantify the variation in the values of FI-related parameters under non-stress conditions. Indeed, in our measured FI curves, the F_v/F_m values were higher than 0.8, implying that we have used healthy, unstressed plants (Björkman and Demmig 1987); furthermore, we did not observe any apparent K phase in the FI induction curve, again suggesting that there was no stress (especially heat) in our plants during our experiments (Strasser et al. 2000; Kalaji et al. 2014; Ripoll et al. 2016) (cf. Fig. 1). Therefore, the data from this study can be used to evaluate the natural variation of FI-related parameters under non-stress conditions.

Based on the measured FI curves, we obtained several quantitative parameters describing FI by using a first-order kinetic equation developed by e.g., Pospíšil and Dau (2000), Boisvert et al. (2006), and Joly and Carpentier (2007). This analysis has provided us a quantitative evaluation of the amplitude and half-time of the O–J, J–I and I–P phases, the

difference of which is usually not easily visually detectable (Boisvert et al. 2006). As an example, by visually inspecting the OJIP FI curves in field grown plants, we could not identify a clear difference between O–J phases for the JAP and IND subpopulations; however, quantitative analysis showed us a clear increase in A_{O-J} of the IND as compared to the JAP subpopulation (Fig. 3c). At the same time, the $t_{1/2}$ of the O–J and J–I phases were also larger in IND compared to that in JAP population (Fig. 3o, s). These results imply that the PQ pool size is not the same in IND and JAP subpopulations, or that there are differences in the PQ pool redox state in darkness, since both affect the occupancy state of the Q_B^-site. A partial reduction of the PQ pool in darkness results in an increased A_{O-J}, since a fraction of the Q_B^-sites will be occupied with PQH_2 instead of PQ at the beginning of the transient (Stirbet et al. 2014) and a reduced PQ can decrease the rate of Q_A^- re-oxidation (de Wijn and van Gorkom 2001). Further, a larger PQ pool will increase the duration of the thermal JIP phase. In addition, results obtained with the JIP test analysis (Strasser et al. 2000), showed that the normalized area above the OJIP curve (S_m), which is proportional to the number of electron acceptors in electron transfer chain (e.g., Strasser et al. 2000; Bennoun 2001), was considerably larger in IND as compared to JAP population (Fig. 4g), implying a larger PQ pool size in the IND population, which may explain the slower rate of complete reduction of PQ pool in this subpopulation. However, there might be other additional possibilities (e.g., see Joliot and Joliot 2002; Schansker et al. 2005; Toth et al. 2007). Moreover, the maximum quantum yield of PSII photochemistry (F_v/F_m) in IND was clearly lower than in JAP, while the apparent antenna size of an active PSII (ABS/RC) was similar in both IND and JAP. As a result, the performance index PI_{abs}, which depends on ABS/RC, $F_v/F_m = \varphi_{Po}$, and the efficiency with which a PSII trapped electron is transferred from Q_A^- to Q_B (i.e., ψ_{Eo}; see Table 1), was also clearly lower in IND than in JAP (Fig. 4c).

In essence, there is a general agreement on the meaning of the I–P phase, which has been suggested to be related to the reduction of electron transport carriers on the (electron) acceptor side of PSI, as well as to a transient block of electron transfer on the (electron) acceptor side of PSI (Munday and Govindjee1969; Satoh 1981; Schansker et al. 2003, 2006; Hamdani et al. 2015). Also, it has been shown that, under certain conditions, A_{I-P} can be correlated with the amount of PSI (Ceppi et al. 2012), and that, theoretically, variable PSI fluorescence may contribute in a small proportion to this phase (Lazár 2006). Here, we find that there is a higher A_{I-P} in JAP than IND accessions (Fig. 3k); although this could have multiple causes, one possibility is that PSI/PSII ratio is higher in JAP than in IND plants (see e.g., Ceppi et al. 2012). Further research is needed to understand this difference (also see below). In addition, Soda et al. (2018) have shown that over-expression of OsIF (rice intermediate filament) increased A_{I-P} together with an increased biomass production. The mechanistic basis underlying this correlation is still unknown.

Relationship between FI-related parameters in rice accessions and environmental parameters for the origin of these accessions

The impact of short- or long-term environmental treatment on FI-related parameters have been studied by several researchers (see e.g., Kalaji et al. 2014; Jedmowski et al. 2015; Živčák et al. 2015; Wungrampha et al. 2019). These, and many other studies, have improved our understanding of the responses or acclimation of photosynthetic systems, in particular components of the photosynthetic light reactions, to environmental factors. Most of these studies have used a limited number of plant species or crop cultivars; hence the conclusions drawn might be species specific or cultivar specific. With the climatic parameters for the origin of each rice cultivar available, the collected FI curves, shown in this paper, and also the derived parameters for all these cultivars make it possible to evaluate the potential generic impact of long-term environmental treatment on photosynthetic systems. Here we show that the PAR and mean temperatures are two dominant environmental factors greatly influencing the FI derived parameters, especially the F_v/F_m, the J–I phase and the I–P phase of the OJIP transient (Fig. 5). The F_v/F_m is related to the function of the PSII reaction centers, which has been shown to be negatively correlated with PAR, but positively to the mean temperature (Fig. 5). Since F_v/F_m decreases at high light intensities, and there is a positive correlation of F_v/F_m with temperature (in certain temperature range), this observation might be related to photoinhibition, since both light and temperature are major factors controlling photodamage (Szymańska et al. 2017). However, in addition, light and temperature are also known to modify the composition, function, and structure of the thylakoid membranes (Anderson 1986; Mohanty et al. 2007; Allakhverdiev et al. 2008), and thus the effects are complex.

Among different phases of the OJIP FI curve, the amplitude of the J–I phase is negatively related to PAR, and positively correlated with temperature (Fig. 5). A mechanism underlying such correlation is unknown. Furthermore, we have found here a positive correlation between the amplitude of the I–P phase and PAR, and a negative correlation between the amplitude of the I–P phase with mean temperature (Fig. 5).

Genetic architecture underlies Chl *a* fluorescence parameters

FI curve contains information related to the whole electron transfer chain, which includes the sequential progressive reduction of electron transfer intermediates in PSII cytochrome (Cyt) b_6/f complex, and in PSI, up to ferredoxin (Fd), since the ferredoxin–NADP + -reductase (FNR) in plants is inactive up to 1–2 s (s) after the onset of illumination (see e.g., Schansker et al. 2005; Govindjee et al. 2017). There are large variations in FI curves and in the derived quantitative parameters under non-stress conditions (Table 2; Fig. 2). Furthermore, there are substantial phenotypic variations within subpopulations of rice, strongly implying that the rice minicore diversity panel can be potentially used to study the genetic basis underlying the variations of OJIP in FI curves. To further confirm that this minicore diversity panel can be used to study the genetic basis of the OJIP FI curve, we have conducted, in this research, SNP heritability analysis (see Table 2). We have indeed found that although the *ħ2* values were very small for most traits, they were statistically significant, especially for the parameters derived from the data collected in field grown rice (Table 2). The highest *ħ2* obtained in this study is for F_v/F_m and F_v/F_o (i.e., 0.32), which is consistent with earlier reports (Herritt et al. 2018; Lin et al. 2018). These significant *ħ2* values, observed for different Chl *a* fluorescence parameters, imply that the genes controlling these parameters can indeed be determined (Ackerly et al. 2000).

With the above information in hand, we have conducted a genome-wide association study (GWAS) for several parameters associated with FI. We note that in the past few years, GWAS has been used to study the genetic architecture underlying FI parameters for different species, including soybean, barley, rice, and Arabidopsis (van Rooijen et al. 2015; Wang et al. 2017; Herritt et al. 2018; Oyiga et al. 2019; Rapacz et al. 2019; Tsai et al. 2019; Quero et al. 2020). In our current paper, we have not only identified the significant loci for each of the studied parameters, but we have further used linkage disequilibrium (LD) analysis to identify all the potential genes associated with lead SNP, which appeared common in at least two parameters within the same LD block (Table 4 and Table S2 under supplementary file 1). It was not the purpose of this study to pinpoint the genes controlling individual parameters; however, here, we have made a beginning. Specifically, we have identified common lead SNPs, which are associated with highly correlated parameters, summarized in Table S1 under supplementary file 1. Earlier studies have shown that parameters highly correlated with each other (positive or negative) might be under similar genetic control (Yang et al. 2007; Yin et al. 2010). Our analysis here has shown that a similar genetic region is associated with F_v/F_m and F_v/F_o, which has given us the highest correlation ($r = 0.98$). Similar genomic regions were also found to be associated with the following pairs: ABS/RC & PI_{abs}; and A_{J-I} & A_{I-P}, which were negatively correlated with each other (Table 3; Figs. 2, 6).

We have further identified potential genes within the shared lead SNPs. There are a number of known photosynthesis genes within the LD block harboring the shared lead SNPs (Table 4). Further studies are needed to establish the genetic relationship between these genes and the associated FI-related parameters. We emphasize that our GWAS analysis has already identified a number of genes that are shown to be related to photosystem structure and function. For example, psb28, a protein involved in the biogenesis of the PSII inner antenna CP47 in cyanobacterium Synechocystis sp. PCC 6803 (Dobáková et al. 2009), is shown to be related to F_v/F_m (Table 4). Similarly, LOC_Os09g12540, which is a light harvesting complex-related gene in rice, was found to be associated with ABS/RC (Table 4; Umate 2010); which is logical since changes in the structure and function of light harvesting complex in principle should change the antenna size, as indicated by ABS/RC. The OsPsbR1, which is a gene potentially involved in the assembly of OEC protein PsbP, and plays a role in cold stress signal transduction (Li et al. 2016), was shown here to be related to F_v/F_m (Table 4). We emphasize that these three proteins, i.e., psb28, protein coded by LOC_Os09g12540, and OsPsbR1, were identified here solely based on the genome-wide association with their corresponding FI-related signals, i.e., these proteins should directly influence the electron transfer process in PSII. More detailed mechanistic studies are needed to reveal how these genes, and also the other newly identified genes influence electron transfer in PSII and even in PSI.

Recently, Hamdani et al. (2019) have found that β-glu5 gene (LOC_Os01g70520), which is involved in the gibberellic acid (GA) pathway, is a major factor controlling variations in F_v/F_m. Here, we find another gene LOC_Os01g08220, which was implicated in GA pathway (Itoh et al. 2001), to be associated with the A_{J-I} and A_{I-P} of the OJIP curve. These together support the notion that the GA metabolism can influence photosynthetic light reactions. In agreement with this, Li et al (2018) showed that GRF4, a transcription factor, can physically interact with DELLA, a protein in the GA signaling pathway, to regulate expression of photosynthesis light reaction-related proteins.

In summary, under defined conditions, our current study provides a comprehensive survey of the natural variations in the Chl *a* fluorescence induction curve in a rice minicore diversity panel. However, further investigation is needed under different sets of environmental conditions in order to determine the sensitivity of the studied phenotype to establish precise identification of expression of genetic variation influenced by the environment. We have, indeed,

found significant variations in FI parameters among different subpopulations of rice. We have found that F_v/F_m, A_{J-I}, and A_{I-P} show strong correlation with climatic parameters, in particular, the photosynthetic active radiation and mean temperature of the region where the cultivar was bred or grown. Parameters measured in plants under field condition (FC) are under strong genetic control compared to the same parameters measured on plants grown in growth chambers (GC). Using GWAS, i.e., *genome-wide association analysis*, we have identified significant genomic loci related to different FI-related parameters. Many loci shared by multiple FI-related parameters have been identified as well in our study. The significant GWAS signal identified here can be used to identify new genes controlling different phases of the FI curve, and thus identify novel genes controlling energy and electron transfer processes in photosynthetic light reactions.

Acknowledgements This work was sponsored by Strategic Priority Research Program of the Chinese Academy of Sciences (Grant No. XDB27020105), National Science Foundation of China (31870214), National Research and Development Program of Ministry of Science and Technology of China (2019YFA0904600; 2019YFA09004600). Govindjee thanks the staff of the Information Technology of Life Sciences, University of Illinois at Urbana-Champaign, for help. We thank members of Prof. Chengcai Chu's lab for plant growth support for experiments done in Beijing. The study was sponsored by CAS-TWAS President's Ph.D. Fellowship Program (to Naveed Khan) for international Ph.D. students.

Author contributions NK, SH, and XZ conceived and conducted the experiments; NK and SH performed most of the experiments, MQ, ML, JE, SP, and XZ provided technical assistance to NK and NK analyzed the data; GG and XZ supervised the experiments; NK wrote most of the text; JE, GG, AS and XZ supervised and complemented the writing of this manuscript.

Compliance with ethical standards

Conflict of interest The authors declare that they have no conflict of interest.

References

Ackerly DD, Dudley SA, Sultan SE, Schmitt J, Coleman JS, Linder CR, Sandquist DR, Geber MA, Evans AS, Dawson T, Lechowicz ML (2000) The evolution of plant ecophysiological traits: recent advances and future directions. Bioscience 50:979–995

Agrama HA, Yan W, Jia M, Fjellstrom R, McClung AM (2010) Genetic structure associated with diversity and geographic distribution in the USDA rice world collection. Nat Sci 2:247–291

Allakhverdiev SI, Kreslavski VD, Klimov VV, Los DA, Carpentier R, Mohanty P (2008) Heat stress: an overview of molecular responses in photosynthesis. Photosynth Res 98:541–550

Anderson JM (1986) Photoregulation of the composition, function, and structure of thylakoid membranes. Annu Rev Plant Biol 37:93–136

Bennoun P (2001) Chlororespiration and the process of carotenoid biosynthesis. Biochim Biophys Acta 1506:133–142

Björkman O, Demmig B (1987) Photon yield of O_2 evolution and chlorophyll fluorescence characteristics at 77 K among vascular plants of diverse origins. Planta 170:489

Boisvert S, Joly D, Carpentier R (2006) Quantitative analysis of the experimental O-J–I–P chlorophyll fluorescence induction kinetics: apparent activation energy and origin of each kinetic step. FEBS J 273:4770–4777

Brachi B, Morris GP, Borevitz JO (2011) Genome-wide association studies in plants: the missing heritability is in the field. Genome Biol 12:232

Bukhov NG, Egorova EA, Govindachary S, Carpentier R (2004) Changes in polyphasic chlorophyll a fluorescence induction curve upon inhibition of donor or acceptor side of photosystem II in isolated thylakoids. Biochim Biophys Acta 1657:121–130

Butler WL (1972) On the primary nature of fluorescence yield changes associated with photosynthesis. Proc Natl Acad Sci USA 69:3420–3422

Butler WL (1978) Energy distribution in the photochemical apparatus of photosynthesis. Annu Rev Plant Physiol 29:345–378

Ceppi MG, Oukarroum A, Çiçek N, Strasser RJ, Schansker G (2012) The IP amplitude of the fluorescence rise OJIP is sensitive to changes in the photosystem I content of leaves: a study on plants exposed to magnesium and sulfate deficiencies, drought stress and salt stress. Physiol Plant 144:277–288

Çiçek N, Oukarroum A, Strasser RJ, Schansker G (2018) Salt stress effects on the photosynthetic electron transport chain in two chickpea lines differing in their salt stress tolerance. Photosynth Res 136:291–301

Dai Y, Shen Z, Liu Y, Wang L, Hannaway D, Lu H (2009) Effects of shade treatments on the photosynthetic capacity, chlorophyll fluorescence, and chlorophyll content of *Tetrastigma hemsleyanum* Diels et Gilg. Environ Exp Bot 65:177–182

De Wijn R, van Gorkom HJ (2001) Kinetics of electron transfer from Q_A to Q_B in photosystem II. Biochemistry 40:11912–11922

Delosme R, Joliot P (2002) Period four oscillations in chlorophyll *a* fluorescence. Photosynth Res 73:165–168

Doerge RW (2002) Mapping and analysis of quantitative trait loci in experimental populations. Nat Rev Genet 3:43–52

Dobáková M, Sobotka R, Tichý M, Komenda J (2009) Psb28 protein is involved in the biogenesis of the Photosystem II inner antenna CP47 (PsbB) in the cyanobacterium *Synechocystis* sp. PCC 6803. Plant Physiol 149:1076–1086

Driever SM, Simkin AJ, Alotaibi S, Fisk SJ, Madgwick PJ, Sparks CA, Jones HD, Lawson T, Parry MA, Raines CA (2017) Increased SBPase activity improves photosynthesis and grain yield in wheat grown in greenhouse conditions. Philos Trans R Soc B 372:1–10

Genty B, Wonders J, Baker NR (1990) Non-photochemical quenching of Fo in leaves is emission wavelength dependent: consequences for quenching analysis and its interpretation. Photosynth Res 26:133–139

Gibson G (2010) Hints of hidden heritability in GWAS. Nat Genet 42:558–560

Goedheer JC (1972) Fluorescence in relation to photosynthesis. Annu Rev Plant Physiol (now Biol) 87:1–12

Govindjee [G] (1995) Sixty-three years since Kautsky: chlorophyll a fluorescence. Austral J Plant Physiol (now Funct Plant Biol) 22:131–160

Govindjee [G] (2004) Chlorophyll a fluorescence: a bit of basics and history. In: Papageorgiou G, Govindjee (eds) Chlorophyll a fluorescence: a probe of photosynthesis. Kluwer Academic Publishers (now Springer). Dordrecht, Netherlands, pp 2–42

Govindjee G, Amesz J, Fork DC (eds) (1986) Light emission by plants and bacteria. Academic Press, Orlando

Govindjee G, Shevela D, Björn L (2017) Evolution of the Z-scheme of photosynthesis: a perspective. Photosynth Res 133:5–15

Gu J, Yin X, Stomph TJ, Struik PC (2014) Can exploiting natural genetic variation in leaf photosynthesis contribute to increasing rice productivity? A simulation analysis. Plant Cell Environ 37:22–34

Guo Y, Tan J (2015) Recent advances in the application of chlorophyll *a* fluorescence from Photosystem II. Photochem Photobiol 91:1–14

Hamdani S, Qu M, Xin C-P, Li M, Govindjee G, Chu C, Zhu X-G (2015) Variations between the photosynthetic properties of elite and landrace Chinese rice cultivars revealed by simultaneous measurements of 820 nm transmission signal and chlorophyll *a* fluorescence induction. J Plant Physiol 177:128–138

Hamdani S, Wang H, Zheng G, Perveen S, Qu M, Khan N, Khan W, Jiang J, Li M, Liu X, Zhu X, Govindjee G, Chu C, Zhu X-G (2019) Genome-wide association study identifies variation of glucosidase being linked to natural variation of the maximal quantum yield of photosystem II. Physiol Plant 166:105–119

Hao D, Chao M, Yin Z, Yu D (2012) Genome-wide association analysis detecting significant single nucleotide polymorphisms for chlorophyll and chlorophyll fluorescence parameters in soybean (Glycine max) landraces. Euphytica 186:919–931

Herritt M, Dhanapal AP, Purcell LC, Fritschi FB (2018) Identification of genomic loci associated with 21 chlorophyll fluorescence phenotypes by genome-wide association analysis in soybean. BMC Plant Biol 312:1–19

Hoffman GE (2013) Correcting for population structure and kinship using the linear mixed model: theory and extensions. PLoS ONE 8:e75707

Huang X, Sang T, Zhao Q, Feng Q, Zhao Y, Li C, Zhu C, Lu T, Zhang Z, Li M (2010) Genome-wide association studies of 14 agronomic traits in rice landraces. Nat Genet 42:961–967

Huang X, Zhao Y, Li C, Wang A, Zhao Q, Li W, Guo Y, Deng L, Zhu C, Fan D (2012) Genome-wide association study of flowering time and grain yield traits in a worldwide collection of rice germplasm. Nat Genet 44:32–39

Itoh H, Ueguchi-Tanaka M, Sentoku N, Kitano H, Matsuoka M, Kobayashi M (2001) Cloning and functional analysis of two gibberellin 3β-hydroxylase genes that are differently expressed during the growth of rice. Proc Natl Acad Sci USA 98:8909–8914

Jedmowski C, Ashoub A, Momtaz O, Brüggemann W (2015) Impact of drought, heat, and their combination on chlorophyll fluorescence and yield of wild barley (*Hordeum spontanum*). J Bot 120868:1–9

Jimenez-Francisco B, Stirbet A, Aguado-Santacruz GA, Campos H, Conde-Martinez FV, Padilla-Chacon D, Trejo C, Bernacchi CJ, Govindjee G (2019) A comparative chlorophyll a fluorescence study on isolated cells and intact leaves of *Bouteloua gracilis* (blue grama grass). Photosynthetica 57:77–89

Joliot P, Joliot A (2002) Cyclic electron transfer in plant leaf. Proc Natl Acad Sci USA 99:10209–102014

Joly D, Carpentier R (2007) The oxidation/reduction kinetics of the plastoquinone pool controls the appearance of the I-peak in the O-J–I–P chlorophyll fluorescence rise: effects of various electron acceptors. J Photochem Photobiol B 88:43–50

Kalaji HM, Carpentier R, Allakhverdiev SI, Karolian B (2012) Fluorescence parameters as early indicators of light stress in barley. J Photochem Photobiol B 112:1–6

Kalaji HM, Schansker G, Ladle RJ, Goltsev V, Bosa K, Allakhverdiev SI, Brestic M, Bussotti F, Calatayud A, Dabrowski P, Elsheery NI, Ferroni L, Guidi L, Hogewoning SW, Jajoo A, Misra AN, Nebauer SG, Pancaldi S, Penella C, Poli D, Pollastrini M, Romanowska-Duda ZB, Rutkowska B, Serôdio J, Suresh K, Szulc W, Tambussi E, Yanniccari M, Zivcak M (2014) Frequently asked questions about in vivo chlorophyll fluorescence: practical issues. Photosynth Res 122:121–158

Kalaji HM, Schansker G, Brestic M, Bussotti F, Calatayud A, Ferroni L, Goltsev V, Guidi L, Jajoo A, Li P, Losciale P, Mishra VK, Misra AN, Nebauer SG, Pancaldi S, Penella C, Pollastrini M, Suresh K, Tambussi E, Yanniccari M, Zivcak M, Cetner MD, Samborska IA, Stirbet A, Olsovska K, Kunderlikova K, Shelonzek H, Rusinowski S, Bąba W (2017) Frequently asked questions about chlorophyll fluorescence, the sequel. Photosynth Res 132:13–66

Goltsev VN, Kalaji HM, Paunov M, Baba V, Horaczek T, Moyski J, Kozel H, Allakhverdiev SI (2016) Variable chlorophyll fluorescence and its use for assessing physiological condition of plant photosynthetic apparatus. Russ J Plant Physiol 63:871–895

Kasajima I, Ebana K, Yamamoto T, Takahara K, Yano M, Kawai-Yamada M, Uchimiya H (2011) Molecular distinction in genetic regulation of nonphotochemical quenching in rice. Proc Natl Acad Sci USA 108:13835–13840

Kautsky H, Hirsch A (1931) Neue Versuche zur Kohlensäureassimilation. Naturwissenschaften 19:964

Kump KL, Bradbury PJ, Wisser RJ, Buckler ES, Belcher AR, Oropeza-Rosas MA, Zwonitzer JC, Kresovich S, McMullen MD, Ware D (2011) Genome-wide association study of quantitative resistance to southern leaf blight in the maize nested association mapping population. Nat Genet 43:163–168

Lazár D (2003) Chlorophyll a fluorescence rise induced by high light illumination of dark-adapted plant tissue studied by means of a model of photosystem II and considering photosystem II heterogeneity. J Theor Biol 220:469–503

Lazár D (2006) The polyphasic chlorophyll *a* fluorescence rise measured under high intensity of exciting light. Funct Plant Biol 33:9–30

Li X, Yan W, Agrama H, Hu B, Jia L, Jia M, Jackson A, Moldenhauer K, McClung A, Wu D (2010) Genotypic and phenotypic characterization of genetic differentiation and diversity in the USDA rice mini-core collection. Genetica 138:1221–1230

Li L, Ye T, Gao X, Chen R, Xu J, Xie C, Zhu J, Deng X, Wang P, Xu Z (2016) Molecular characterization and functional analysis of the OsPsbR gene family in rice. Mol Genet Genomics 292:271–281

Li S, Tian Y, Wu K, Ye Y, Yu J, Zhang J, Liu Q, Hu M, Li H, Tong Y, Harberd NP, Fu X (2018) Modulating plant growth–metabolism coordination for sustainable agriculture. Nature 560:595–600

Lin D, Zheng K, Liu Z, Li Z, Teng S, Xu J, Dong Y (2018) Rice TCM1 encoding a component of the TAC complex is required for chloroplast development under cold stress. Plant Genome 11:1–13

Mehta P, Allakhverdiev SI, Jajoo A (2010) Characterization of photosystem II heterogeneity in response to high salt stress in wheat leaves (Triticum aestivum). Photosynth Res 105:249–255

Mishra M, Wungrampha S, Kumar G, Singla-Pareek SL, Pareek A (2020) How do rice seedlings of landrace Pokkali survive in saline fields after transplantation? Physiology, biochemistry, and photosynthesis. Photosynth Res. https://doi.org/10.1007/s11120-020-00771-6

Mohanty P, Allakhverdiev SI, Murata N (2007) Application of low temperatures during photoinhibition allows characterization of individual steps in photodamage and the repair of photosystem II. Photosynth Res 94:217–224

Munday JC Jr, Govindjee G (1969) Light-induced changes in the fluorescence yield of chlorophyll *a* in vivo: III. The dip and the peak in the fluorescence transient of *Chlorella pyrenoidosa*. Biophys J 9:1–21

Neubauer C, Schreiber U (1987) The polyphasic rise of chlorophyll fluorescence upon onset of strong continuous illumination: I. Saturation characteristics and partial control by the photosystem II acceptor side. Z Naturforsch 42c:1246–1254

Oyiga BC, Ogbonnaya FC, Sharma RC, Baum M, Léon J, Ballvora A (2019) Genetic and transcriptional variations in NRAMP-2 and OPAQUE1 genes are associated with salt stress response in wheat. Theor Appl Genet 132:323–346

Oukarroum A, El Madidi S, Strasser RJ (2016) Differential heat sensitivity index in barley cultivars (*Hordeum vulgare* L.) monitored by chlorophyll *a* fluorescence OKJIP. Plant Physiol Biochem 105:102–108

Papageorgiou GC, Govindjee G (eds) (2004) Chlorophyll *a* fluorescence: a signature of photosynthesis. Springer, Dordrecht

Papageorgiou GC, Govindjee G (2011) Photosystem II fluorescence: slow changes - Scaling from the past. J Photochem Photobiol B 104:258–270

Pfündel E (1998) Estimating the contribution of Photosystem I to total leaf chlorophyll fluorescence. Photosynth Res 56:185–195

PospíšilP DH (2000) Chlorophyll fluorescence transients of photosystem II membrane particles as a tool for studying photosynthetic oxygen evolution. Photosynth Res 65:41–52

Qu M, Zheng G, Hamdani S, Essemine J, Song Q, Wang H, Chu C, Sirault X, Zhu X-G (2017) Leaf photosynthetic parameters related to biomass accumulation in a global rice diversity survey. Plant Physiol 175:248–258

Quero G, Bonnecarrère V, Simondi S, Santos J, Fernández S, Gutierrez L, Garaycochea S, Borsani O (2020) Genetic architecture of photosynthesis energy partitioning as revealed by a genome-wide association approach. Photosynth Res. https://doi.org/10.1007/s11120-020-00721-2

Rapacz M, Wójcik-Jagła M, Fiust A, Kalaji HM, Koscielniak J (2019) Genome-wide associations of chlorophyll fluorescence OJIP transient parameters connected with soil drought response in barley. Front Plant Sci 10:78

Ripoll J, Bertin N, Bidel LP, Urban L (2016) A user's view of the parameters derived from the induction curves of maximal chlorophyll a fluorescence: perspectives for analyzing stress. Front Plant Sci 7:1679

Satoh K (1981) Fluorescence induction and activity of ferredoxin-NADP+ reductase in Bryopsis chloroplasts. Biochim Biophys Acta 638:327–333

Schansker G, Srivastava A, Govindjee G, Strasser RJ (2003) Characterization of the 820-nm transmission signal paralleling the chlorophyll a fluorescence rise (OJIP) in pea leaves. Funct Plant Biol 30:785–796

Schansker G, Tóth SZ, Strasser RJ (2005) Methylviologen and dibromothymoquinone treatments of pea leaves reveal the role of photosystem I in the Chl *a* fluorescence rise OJIP. Biochim Biophys Acta 1706:250–261

Schansker G, Tóth SZ, Strasser RJ (2006) Dark recovery of the Chl *a* fluorescence transient (OJIP) after light adaptation: The qT-component of non-photochemical quenching is related to an activated photosystem I acceptor side. Biochim Biophys Acta 1757:787–879

Schansker G, Tóth SZ, Kovacs L, Holzwarth AR, Garab G (2011) Evidence for a fluorescence yield change driven by a light-induced conformational change within photosystem II during the fast chlorophyll a fluorescence rise. Biochim Biophys Acta 1807:1032–1043

Schläppi MR, Jackson AK, Eizenga GC, Wang A, Chu C, Shi Y, Shimoyama N, Boykin DL (2017) Assessment of five chilling tolerance traits and GWAS mapping in rice using the USDA mini-core collection. Front Plant Sci 8:957

Schreiber U, Vidaver W (1976) The ID fluorescence transient. An indicator of rapid energy distribution changes in photosynthesis. Biochim Biophys Acta 440:205–214

Schreiber U (1986) Detection of rapid induction kinetics with a new type of high-frequency modulated chlorophyll fluorometer. Photosynth Res 9:261–272

Schreiber U, Neubauer C (1987) The polyphasic rise of chlorophyll fluorescence upon onset of strong continuous illumination: II. Partial control by the photosystem II donor side and possible ways of interpretation. Z Naturforsch C 42:1255–1264

Shinkarev VP, Govindjee G (1993) Insight into the relationship of chlorophyll *a* fluorescence yield to the concentration of its natural quenchers in oxygenic photosynthesis. Proc Natl Acad Sci USA 90:7466–7469

Soda N, Gupta BK, Anwar K, Sharan A, Govindjee G, Singla-Pareek SL, Pareek A (2018) Rice Intermediate Filament, OsIF, stabilizes photosynthetic machinery and yield under salinity and heat stress. Sci Rep 8:4072

Stirbet A, Govindjee G (2011) On the relation between the Kautsky effect (chlorophyll *a* fluorescence induction) and photosystem II: basics and applications of the OJIP fluorescence transient. J Photochem Photobiol B 104:236–257

Stirbet A, Govindjee G (2012) Chlorophyll *a* fluorescence induction: a personal perspective of the thermal phase, the J-I-P rise. Photosynth Res 113:15–61

Stirbet A, Riznichenko GY, Rubin AB, Govindjee. (2014) Modeling chlorophyll *a* fluorescence transient: relation to photosynthesis. Biochemistry (Mosc) 79:291–323

Stirbet A, Govindjee G (2016) The slow phase of chlorophyll *a* fluorescence induction in silico: origin of the S-M fluorescence rise. Photosynth Res 130:193–213

Stirbet A, Lazár D, Kromdijk J, Govindjee G (2018) Chlorophyll *a* fluorescence induction: Can just a one second measurement be used to quantify abiotic stress responses? Photosynthetica 56:86–104

Strasser RJ, Govindjee G (1992) The Fo and the O-J-I-P fluorescence rise in higher plants and algae. In: Argyroudi-Akoyunoglou JH (ed) Regulation of chloroplast biogenesis. Plenum Press, New York, pp 423–426

Strasser RJ, Srivastava A, Govindjee G (1995) Polyphasic chlorophyll *a* fluorescence transient in plants and cyanobacteria. Photochem Photobiol 61:32–42

Strasser RJ, Srivastava A, Tsimilli-Michael M (2000) The fluorescence transient as a tool to characterize and screen photosynthetic samples. In: Yunus M, Pathre U, Mohanty P (eds) Probing photosynthesis: mechanisms, regulation and adaptation. Taylor & Francis, London, pp 445–483

Strasser RJ, Tsimilli-Michael M, Srivastava A (2004) Analysis of the chlorophyll *a* fluorescence transient. In: G.C. Papageorgiou and Govindjee (eds.) Chlorophyll a fluorescence: a probe of photosynthesis. Kluwer Academic (now Springer). Dordrecht. pp 321–362

Sun Y, Zhang Z, Xu C, Shen C, Gao C, Wang L (2009) Effect of ALA on fast chlorophyll fluorescence induction dynamics of watermelon leaves under chilling stress. Acta Hortic Sin 36:671–678

Szymańska R, Ślesak I, Orzechowska A, Kruk J (2017) Physiological and biochemical responses to high light and temperature stress in plants. Environ Exp Bot 139:165–177

Tian F, Bradbury PJ, Brown PJ, Hung H, Sun Q, Flint-Garcia S, Rocheford TR, McMullen MD, Holland JB, Buckler ES (2011) Genome-wide association study of leaf architecture in the maize nested association mapping population. Nat Genet 43:159–162

Tóth SZ, Schansker G, Strasser RJ (2007) A non-invasive assay of the plastoquinone pool redox state based on the OJIP-transient. Photosynth Res 93:193–203

Tsai Y-C, Chen K-C, Cheng T-S, Lee C, Lin S-H, Tung C-W (2019) Chlorophyll fluorescence analysis in diverse rice varieties reveals the positive correlation between the seedlings salt tolerance and photosynthetic efficiency. BMC Plant Biol 19:403

Tsimilli-Michael M (2020) Revisiting JIP-test: an educative review on concepts, assumptions, approximations, definitions and terminology. Photosynthetica 58:275–292

Turner SD (2018) qqman: an R package for visualizing GWAS results using QQ and Manhattan plots. J Open Source Softw 3:731–732
Umate P (2010) Genome-wide analysis of the family of light-harvesting chlorophyll a/b-binding proteins in Arabidopsis and rice. Plant Signal Behav 5:1537–1542
van Rooijen R, Harbinson J, Aarts M (2015) Natural genetic variation for acclimation of photosynthetic light use efficiency to growth irradiance in *Arabidopsis*. Plant Physiol 167:1412–1429
Wang D, Sun Y, Stang P, Berlin JA, Wilcox MA, Li Q (2009) Comparison of methods for correcting population stratification in a genome-wide association study of rheumatoid arthritis: principal-component analysis versus multidimensional scaling. BMC Proc 3(Suppl 7):1–6
Wang H, Xu X, Vieira FG, Xiao Y, Li Z, Wang J, Nielsen R, Chu C (2016) The power of inbreeding: NGS-based GWAS of rice reveals convergent evolution during rice domestication. Mol Plant 9:975–985
Wang Q, Xie W, Xing H, Yan J, Meng X, Li X, Fu X, Xu J, Lian X, Yu S (2015) Genetic architecture of natural variation in rice chlorophyll content revealed by a genome-wide association study. Mol Plant 8:946–957
Wang Q, Zhao H, Jiang J, Xu J, Xie W, Fu X, Liu C, He Y, Wang G (2017) Genetic architecture of natural variation in rice nonphotochemical quenching capacity revealed by genome-wide association study. Front Plant Sci 8:1773
Wungrampha S, Joshi R, Rathore RS, Singla-Pareek SL, Govindjee G, Pareek A (2019) CO_2 and chlorophyll *a* fluorescence of *Suaeda fruticosa* grown under diurnal rhythm and after transfer to continuous dark. Photosynth Res 142:211–227
Yan J, Shah T, Warburton ML, Buckler ES, McMullen MD, Crouch J (2009) Genetic characterization and linkage disequilibrium estimation of a global maize collection using SNP markers. PLoS ONE 4:e8451
Yang DL, Jing RL, Chang XP, Li W (2007) Quantitative trait loci mapping for chlorophyll fluorescence and associated traits in wheat (*Triticum aestivum*). J Int Plant Biol 49:646–654
Yang J, Lee SH, Goddard ME, Visscher PM (2011) GCTA: a tool for genome-wide complex trait analysis. Am J Hum Genet 88:76–82
Yin Z, Meng F, Song H, He X, Xu X, Yu D (2010) Mapping quantitative trait loci associated with chlorophyll *a* fluorescence parameters in soybean (*Glycine max* (L.) Merr.). Planta 231:875–885
Zhang M, Shan Y, Kochian L, Strasser RJ, Chen G (2015) Photochemical properties in flag leaves of a super-high-yielding hybrid rice and a traditional hybrid rice (Oryza sativa L.) probed by chlorophyll a fluorescence transient. Photosynth Res 126:275–284
Zhao K, Tung C-W, Eizenga GC, Wright MH, Ali ML, Price AH, Norton GJ, Islam MR, Reynolds A, Mezey J, McClung AM, Bustamante CD, McCouch SR (2011) Genome-wide association mapping reveals a rich genetic architecture of complex traits in Oryza sativa. Nat Commun 2:467
Zhu XG, Govindjee G, Baker NR, deSturler E, Ort DO, Long SP (2005) Chlorophyll *a* fluorescence induction kinetics in leaves predicted from a model describing each discrete step of excitation energy and electron transfer associated with Photosystem II. Planta 223:114–133
Živčák M, Brestic M, Kalaji HM, Govindjee G (2014) Photosynthetic responses of sun- and shade-grown barley leaves to high light: is the lower connectivity in shade leaves associated with protection against excess of light. Photosynth Res 119:339–354
Živčák M, Olšovská K, Slamka P, Galambošová J, Rataj V, Shao H, Brestič M (2015) Application of chlorophyll fluorescence performance indices to assess the wheat photosynthetic functions influenced by nitrogen deficiency. Plant Soil Environ 60:210–215

Publisher's Note Springer Nature remains neutral with regard to jurisdictional claims in published maps and institutional affiliations.

Affiliations

Naveed Khan[1,2] · Jemaa Essemine[2] · Saber Hamdani[2] · Mingnan Qu[2] · Ming-Ju Amy Lyu[2] · Shahnaz Perveen[2] · Alexandrina Stirbet[3] · Govindjee Govindjee[4] · Xin-Guang Zhu[2]

[1] CAS Key Laboratory of Computational Biology, CAS-MPG Partner Institute for Computational Biology, Institute of Nutrition and Health, University of Chinese Academy of Science, Chinese Academy of Sciences, Shanghai 200031, China

[2] State Key Laboratory for Plant Molecular Genetics and Center of Excellence for Molecular Plant Sciences, Chinese Academy of Sciences, Shanghai 200031, China

[3] Anne Burras Lane, Newport News, VA 23606, USA

[4] Department of Plant Biology, Department of Biochemistry, and Center of Biophysics & Quantitative Biology, University of Illinois at Urbana-Champaign, Urbana, IL 61801, USA